Final Report

Mechanistic investigation of 2-oxo-hept-3-ene-1,7-dioic acid hydratase from *p*-hydroxyphenylacetate degradation pathway of *Acinetobacter baumannii*

By

Asst. Prof. Dr. Pirom Chenprakhon

1 May 2020

Contract No MRG6180156

Final Report

Mechanistic investigation of 2-oxo-hept-3-ene-1,7-dioic acid hydratase from *p*-hydroxyphenylacetate degradation pathway of *Acinetobacter baumannii*

Asst. Prof. Dr. Pirom Chenprakhon
Institute for Innovative Learning
Mahidol University

Project Granted by the Thailand Research Fund

Abstract

Project Code: MRG6180156

Project Title: Mechanistic investigation of 2-oxo-hept-3-ene-1,7-dioic acid hydratase from *p*-hydroxyphenylacetate degradation pathway of *Acinetobacter baumannii*

Investigator: Asst. Prof. Dr. Pirom Chenprakhon

E-mail Address: Pirom.che@mahidol.edu

Project Period: 2 May 2018 – 1 May 2020

Abstract:

Hydratase or hydro-lyase generally catalyzes the addition of a water molecule to a C=C bond and forms an alcohol product. Enzymes in this group catalyze a reaction with high enantio-, regio- and chemo- selectivity that will be useful for the synthesis of stereo-specific alcohols. In this study, OHED hydratase from *A. baumannii* was successfully overexpressed as a soluble recombinant enzyme in *E. coli* expression system using auto-induction media (ZYM). The enzyme could be purified through 3 steps of purification including 0.2% PEI precipitation, 10-30% ammonium sulfate precipitation, and DEAE column chromatography. The oligomeric state of purified OHED hydratase showed the native conformation of decameric enzyme with subunit molecular mass around 29.7 kDa. Optimal temperature and pH of OHED hydratase activity were observed at 40˚C and at pH 7.0, respectively. Metal analysis of OHED hydratase using MP-AES and ICP-OES techniques indicated that various divalent metals were found in the purified enzyme, including Mn^{2+} Zn^{2+} Ca^{2+} and Mg^{2+}. The information from enzyme activity assay using trans-fumarate as substrate and thermal shift assay indicated that Mn^{2+} is a native cofactor of OHED hydratase. Substrate specificity of OHED was investigated using various compounds containing of carbon double bond adjacent to the carboxyl group. The enzyme had high stereo-selectivity as selectively catalyzed only *trans*-fumarate to form L-malate, but was unable to use *cis* form of this compound (maleic acid). The reverse reaction using D/L-malate also revealed that the OHED hydratase only specifically used L-malate as a substrate. Kinetic parameters of forward and reverse reactions were investigated using *trans*-fumarate and L-malate, respectively. The OHED hydratase catalyzes forward reaction more efficiently than the reverse reaction with catalytic efficiency (k_{cat}/K_m) 30-folds higher than that of the reverse reaction.

บทคัดย่อ

เอนไซม์ไฮดราเทส (Hydratase) เร่งปฏิกิริยาการเติมน้ำให้กับสารตั้งต้นที่มีพันธะคู่และได้สารประกอบแอลกอฮอล์เป็นสารผลิตภัณฑ์ เอนไซม์ในกลุ่มนี้เร่งปฏิกิริยาได้อย่างมีความจำเพาะแบบ enantio-, regio- และ chemo- selectivity ซึ่งมีความสำคัญต่อการสังเคราะห์สารประกอบแอลกอฮอล์ที่มีประโยชน์ ในงานวิจัยนี้ได้ทำการผลิตเอนไซม์ไฮดราเทสจากแบคทีเรีย *A. baumannii* (OHED hydratase) โดยทำการแสดงออกของจีน OHED hydratase เพื่อผลิตโปรตีนที่มากเกิน (overexpression) ในระบบของ *E. coli* และทำการแยกเอนไซม์ให้บริสุทธิ์โดย 3 ขั้นตอนคือ การตกตะกอนด้วย PEI (0.2%) การตกตะกอนด้วยเกลือ ammonium sulfate (10-30%) และวิธีทางโครมาโทกราฟีโดยใช้ DEAE column จากการศึกษาพบว่าเอนไซม์ OHED hydratase มีโครงรูปธรรมชาติ (native conformation) เป็นแบบ 10 หน่วยโมโนเมอร์ (decamer) โดยแต่ละหน่วยย่อย (subunit) มีน้ำหนักโมเลกุลเท่ากับ 29.7 kDa สภาวะที่เอนไซม์นี้เร่งปฏิกิริยาได้ดีคืออุณหภูมิ 40 องศาเซลเซียสและค่า pH ที่ 7.0 จากการศึกษาไอออนโลหะในเอนไซม์ด้วยเครื่อง MP-AES และ ICP-OES พบไอออนหลายชนิดที่อาจเป็นโคเฟคเตอร์ (cofactor) ของเอนไซม์ เช่น Mn^{2+} Zn^{2+} Ca^{2+} และ Mg^{2+} แต่จากการข้อมูลของการวัดการทำงานของเอนไซม์ (enzyme assay) และการศึกษา Thermal shift assay ในสถาวะที่มีไอออนโลหะต่างๆ ยืนยันว่า Mn^{2+} เป็นโคเฟคเตอร์ของเอนไซม์ จากนั้นได้ทำการศึกษา substrate specificity โดยใช้สารตั้งต้นชนิดต่างๆที่โครงสร้างโมเลกุลมีพันธะคู่ต่ออยู่กับหมู่คาร์บอกซิล (carboxyl group) พบว่าเอนไซม์มี stereo-selectivity สูง โดยเอนไซม์เร่งปฏิกิริยาใช้ *trans*-fumarate เป็นสารตั้งต้นเท่านั้นและไม่สามารถเร่งปฏิกิริยาใช้ maleic acid ซึ่งเป็น *Cis* isomer ของ *trans*-fumarate ได้ และเมื่อศึกษาการเร่งปฏิกิริยาย้อนกลับ (reverse reaction) โดยใช้ D/L-malate เป็นสารตั้งต้นพบว่าเอนไซม์เร่งปฏิกิริยาได้เฉพาะ L-malate เท่านั้น นอกจากนี้ยังได้ศึกษาและวิเคราะห์หาค่า kinetic parameters ต่างๆของการเร่งปฏิกิริยาของเอนไซม์ OHED hydratase ทั้งปฏิกิริยาไปข้างหน้าโดยใช้ *trans*-fumarate เป็นสารตั้งต้นและปฏิกิริยาย้อนกลับโดยใช้ L-malate เป็นสารตั้งต้น พบว่าประสิทธิภาพการเร่งปฏิกิริยาไปข้างหน้าดีกว่าการเร่งปฏิกิริยาย้อนกลับโดยมีค่า catalytic efficiency (k_{cat}/K_m) มากกว่าประมาณ 30 เท่า

Keywords : Hydratase, 2-oxo-hept-3-ene-1,7-dioic acid hydratase, Metal-dependent enzyme, Acinetobacter baumannii

2. Executive summary

2.1 Introduction to the research problem and its significance

Hydratase or hydro-lyase generally catalyzes addition of a water molecule to a C=C bond and form an alcohol product. This reaction is essential in nature and plays an important role in metabolic pathways such as in the citric acid cycle and fatty acid degradation. Enzymes in this group catalyze reaction with high enantio-, regio- and chemo- selectivity (Wuensch et al., 2013). Therefore, it is attractive for synthesis of chiral alcohols and useful in various applications such as in synthesis of natural products and valuable chemicals compound etc. However, not many applications have been using this enzyme in biocatalysis due to limited knowledge on its reaction mechanism and substrate specificity (Michielsen et al., 2000; Jin and Hanefeld, 2011).

In this proposal, we will overexpress a hydratase from *Acinetobacter baumannii* in *E. coli* system, purify and investigate its biochemical and biophysical properties. Recently, we have identified a gene in the HPA degrading operon that probably encodes for 2-oxo-hepta-3-ene-1,7-dioic acid (OHED) hydratase. We speculate that this gene may encode for the enzyme that catalyzes addition of water into 2-oxo-hept-3-ene-1,7-dioic acid(OHED) and form 2,4-dihydroxy-hept-2-ene-1,7-dioic acid (HHED) (Figure1). However, the product of this gene has never been overexpressed and characterized. Therefore, we propose to characterize biochemical properties of a putative OHED hydratase. The reaction mechanism of OHED hydratase will be investigated using steady-state and pre-steady state kinetics and isotope labeling. We also will investigate amino acid residues that are important for activating H_2O and act as general acid or base in the reaction catalyzed by OHED hydratase. Substrate specificity will also be studied to explore potentials of this enzyme in biocatalytic applications. The information in this study will contribute to a better understanding on reaction mechanisms of the enzyme and will be useful for enzyme engineering to control efficiency and specificity of the enzyme in biocatalysis applications.

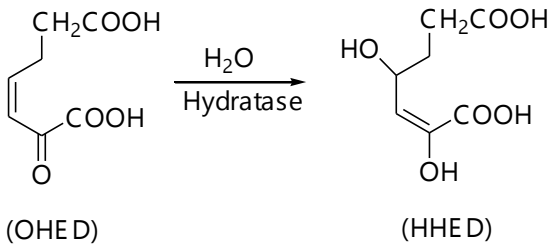

Figure 1. Reaction of catalyzed by OHED hydratase

2.2 Literature review

Hydratase or hydro-lyase catalyzes an addition of water to C=C bond (Figure 2). The enzyme can also catalyze reactions using substrates with C≡C (Liao and Himo, 2011) and C≡N bound (Piersma et al., 2000). In our work, we will focus only on reactions with C=C bonds. The enzymes classified as lyases (E.C.4.2.1-) (Chen et al., 2015) usually catalyze reaction using organic cofactors such as NAD^+ and FAD, and inorganic cofactors such as Mn^{2+} and some of them are cofactor independent (Chen et al., 2015). Hydratase can be grouped into two main groups based on substrates that are isolated (unpolarized) C=C bond and conjugated (polarized) C=C bond (Figure 2). The first group catalyzes addition of water to an isolated (unpolarized) C=C bond. The reaction proceeds via acid-catalyze reaction by having the C=C bond to be protonated first. Then, H_2O acts as a nucleophile to attack onto the double bound. The 1,2 addition of water into an alkene follows the rule of Markonikov in which the hydroxyl group adds to the carbon with more of carbon-carbon bonds. Up to date, many enzymes in this group have been isolated and identified including Kievitone hydratase (E.C.4.2.1.95) (Turbek et al,. 1992), phaseollidin hydratase (E.C.4.2.1.97) (Turbek et al,. 1992), carotenoid 1,2-hydratase (E.C.4.2.1.131) (Maresca et al., 2008), oleate hydratase (E.C.4.2.1.53) (Bevers et al., 2009), limonene hydratease (Bicas et al,. 2010), linalool dehydrogenase-isomerase (Brodkorb et al., 2010). Among of them, oleate hydratase is the most extensively studied. The second group of enzymes catalyze addition of water into a conjugated (polarized) C=C bond. The reaction occurs using acid or base-catalyzed reaction. The substrate C=C bond in conjugated system can be polarized by an electron withdrawing group such as carboxylic acid, ketone, aldehyde and thioesters, making more reactive electrophile and more susceptible by nucleophilic attack by water. Many enzymes in this group have been isolated and identified including malease (E.C.4.2.1.31) (Sacks and Jensen, 1951), 3-dehydroquinate dehydratase (E.C.4.2.1.10) (Hanson and Rose, 1963), fumarase (E.C.4.2.1.2) (Lamartiniere et al., 1970), aconitase (E.C.4.2.1.3) (Beinert et al., 1996), Michael hydratase from *Rhodococus* strain (Halland and Gu, 1998), enoyl-CoA hydratase (E.C.4.2.1.17) (Hiltunen and Qin, 2000), urocanase (E.C.4.2.1.49) (Tyagi et al., 2008) and 3-dehydroshikimate dehydratase (E.C.4.2.1.118) (Pfleger et al., 2008).

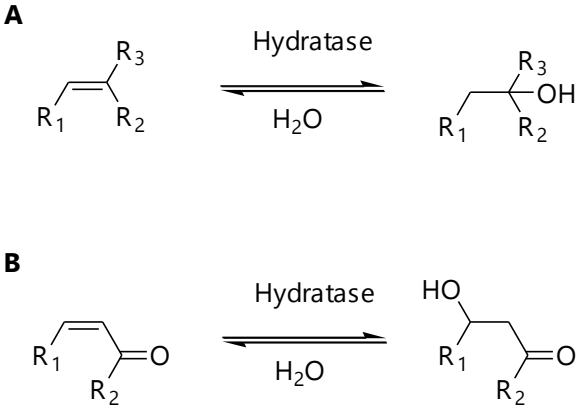

Figure 2. A: Group A hydratase catalyzes water addition to isolated (unpolarized) C=C bond. **B**: Group B hydratase catalyzes water addition to conjugated (polarized) C=C bond.

Both groups of enzyme can catalyze water addition in *syn*- or *anti*- fashion, depending on nature of the enzyme active site. For example, enzymes in the second group such as fumarase, malease, aconitase and Michael hydratase catalyze the *anti*-addition of water to C=C bond whereas enoyl-CoA hydratase catalyzes the *syn*-addition of water to C=C bond. Hydratase-catalyzed reaction is reversible and the equilibrium can lie on either the substrate or product side. For hydratase-catalyzed water addition to isolated (unpolarized) C=C bond, the equilibrium is slightly on the side of substrate while for the reaction of conjugated (polarized) C=C bond, the equilibrium lies on the product side (Chen et al, 2015).

Many hydratases have been reported their mechanistic information and were reviewed by Chen et al, 2015 and Jin and Hanefeld, 2011 (Chen et al, 2015 and Jin and Hanefeld, 2011). Oleate hydratase, fumarase, Malease, Micheal hydratase, aconitase and type II dehydroquinase catalyze the addition of water via *syn*-addition, whereas type I dehydroquinase, enoyl-CoA and artificial hydrotase catalyze reaction via *anti*-addition. Reaction mechanisms of this enzyme were investigated using isotope labeling substrates. For example, in oleate hydratase which is the most extensively studied enzyme that uses isolated (unpolarized) C=C bond as a substrate, the addition of water to C=C bond of oleic acid and produces (R)-10-dihydroxy stearic acid (Figure 3). The reaction mechanism was also investigated by performing the reaction in deuterium oxide (Schroepfer, 1966). As the hydroxyl group deuterium of product is replaced by hydrogen during product purification process, the product with C-9 deuterium-labelled (R)-10-hydroxystearic acid was obtained. The configuration of deuterium labeled at C-9 was investigated by incubating this product in a growing

culture of *Corynecacterium diphtheria*, a system that removed (R)-hydrogen at C-9 carbon of stearic acid (Davis et al. 1969). The product was determined by mass spectrometry and the deuterium still remains in molecule of product, and the reaction identified to be *anti*-addition.

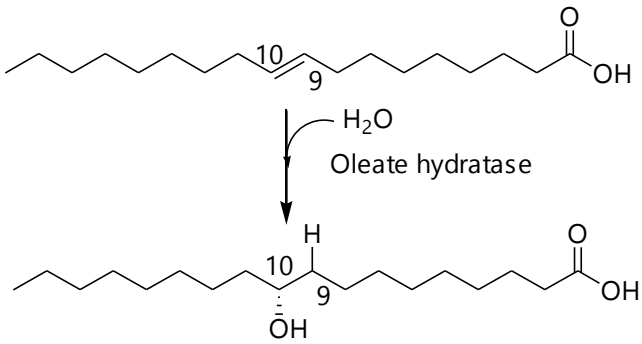

Figure 3. Oleate hydratase catalyses the water addition to oleic acid to form (R)-10-hydroxystearic acid

To date, many crystal structures of hydrotase were obtained including fumarase from C of *E. coli*. (Weaver, 1996), porcine mitochondrial aconitase (Lloyd, 1999), 3-dehydroquinate dehydratase type II (Roszak, 2002), 3-dehydroquinate dehydratase type I and Enoyl-CoA hydratase (Maneiro, 2014). These structural information is useful for understanding enzyme reaction mechanism.

Hydratase in the HPA degradation pathway

In the HPA degradation pathway of *Acinetobacter Baumannii,* 4-HPA is first converted to 3,4-hydroxyphenylacetic acid (homoprotocatechuate) and then several enzymes are involved to generate final metabolites, pyruvate and succinic semialdehyde (Figure 4). Hydratase in the HPA degradation pathway catalyzes addition of water into 2-oxo-hept-3-ene-1,7-dioic acid (OHED) and form 2,4-dihydroxy-hept-2-ene-1,7- dioic acid (HHED) (step7 in Figure 4). However, this enzyme in *Acinetobacter Baumannii* has not been identified and studied.

In the past, several hydratases in HPA degradation pathway and related pathway have been isolated, identified, purified and studied including HpcG (2-oxo-hept-4-ene-1.7-dioate hydratase) in homoprotocatechuate degradation pathway of *Escherichia coli* (Izumi, A. et al, 2007), BphH (2-keto-4-hydroxypentanoate hydratase) in the degradation pathway of biphynyl/chlorobiphenyl from *Burkholderia xenoverans* LB400 (Wang, P. et al, 2005), MhpD (2-hydroxypentadienoic acid hydratase) in the degradation pathway of phenylpropionic acid from *E. coli* (Pollard, J. R. et al, 1998),

GalB (4-carboxy-2-hydroxymuconate hydratase) in the gallate degradation pathway from *Pseudomonas putida* KT2440, (Mazurkewich, S. et al, 2016), LigJ (4-Oxalomesaconate Hydratase) in vanillate and syringate degradation pathway from *Sphingomonas paucimobilis* SYK-6 (Hara, H. et al, 2000), VPH (Vinylpyruvate hydratase) from *Pseudomonas putida* MT-2 and *Leptothrix cholodnii* SP-6 (Johnson, W. H. et al, 2016). All enzymes are divalent metal ion-dependent (Zn^{2+} (GalB and LigJ), Mg^{2+}(HpcG and BphH) and Mn^{2+}(MhpD and VPH)).

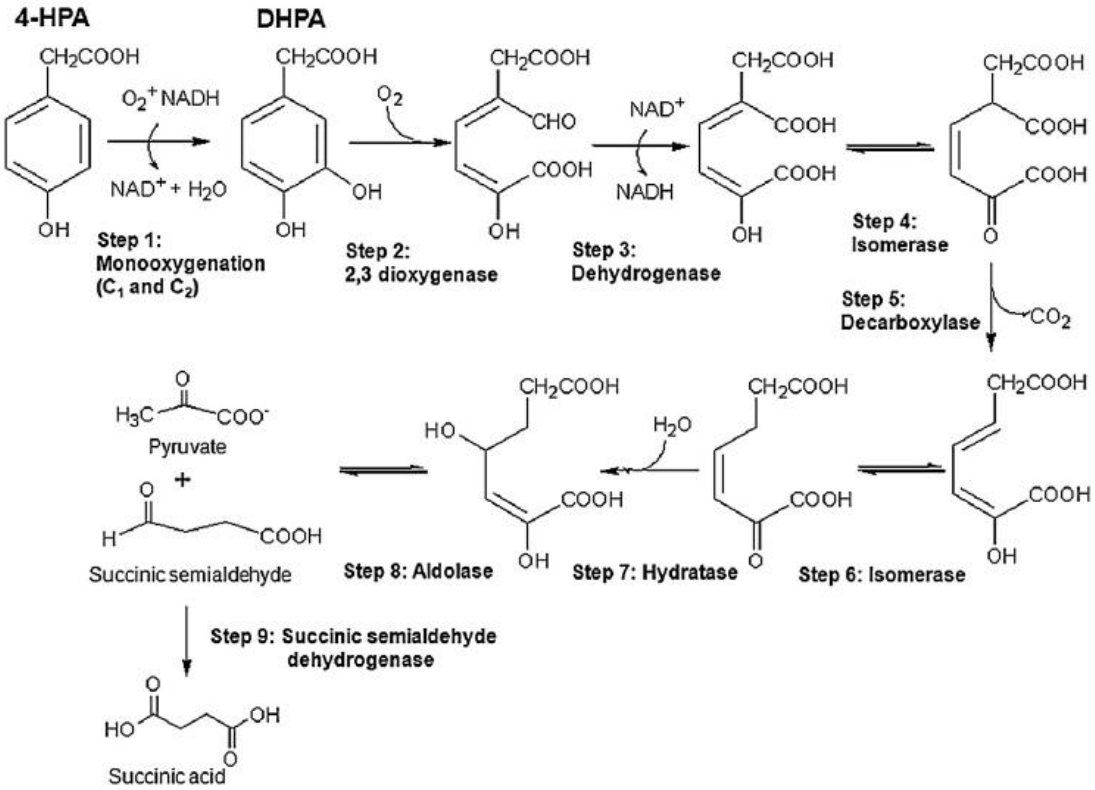

Figure 4. All reactions involved in the HPA degradation to generate pyruvate and succinate as the final metabolites (Thotsaporn et al., 2016).

A few hydratases in HPA and related compounds degradation pathway have been studied including HpcG, VPH, GalB and MhpD. The reaction mechanism of HpcG has been proposed based on the enzyme crystal structure (Izumi et al., 2007) and results from isotopic labeling studies (Burks et al., 1998). In aqueous solution, the substrate is in equilibrium between keto (**1**) and enol (**2**) forms (Figure 5A) and both forms can be used by the enzyme. In the equilibrium mixture, **1** and **2** can also decay to **3** (3E isomer). The double bond to be hydrated should be conjugated with a carbonyl group to facilitate a nucleophilic attack by water. Therefore, compounds **3** (3E isomer**)**

and **4** (3Z isomer) may be intermediates in the reaction catalyzed by HpcG. The evidence from isotopic labeling study (Burks et al., 1998) also suggested that the substrate **1** and **2** can proceed to form the intermediate **3** (3E isomer**)** or **4** (3Z isomer) because the product from the reaction of HpcG in D_2O buffer have deuterium incorporated stereo-specifically at positions C-3 and C-5 (more information in the reaction mechanism depicted in Figure 7). The compound **3** was synthesized and tested and found that it cannot be used by HpcG. Therefore, the compound **3** is not an intermediate for the reaction catalyzed by HpcG and **4** (3Z isomer) should be an intermediate for the reaction catalyzed by HpcG. Studies of MhpD by Pollard and Bugg (Pollard et al., 1998) also found evidence similar to the results of HpcG. In aqueous solution, the substrate of MhpD (2-hydroxy-pentadienoate, **6**) is rapidly ketonized to *trans*-2-ketopent-3-enoate (**7**) (Figure 5B) and the enzyme catalyzes reaction with a poor yield, indicating that **7** is not an intermediate for the MhpD and the intermediate may be *cis*-2-ketopent-3-enoate (**8**). Pollard and Bugg also found that oxalate is a competitive inhibition for MhpD, suggesting that 2-ketopent-3-enoate may be an intermediate during the reaction of MhpD. Although studies of HpcG and MhpD proposed that the enzyme catalyzes the reaction through the intermediate 3Z, there is no solid evidence to support this proposal because the intermediates **4** and **8** have not been synthesized and tested.

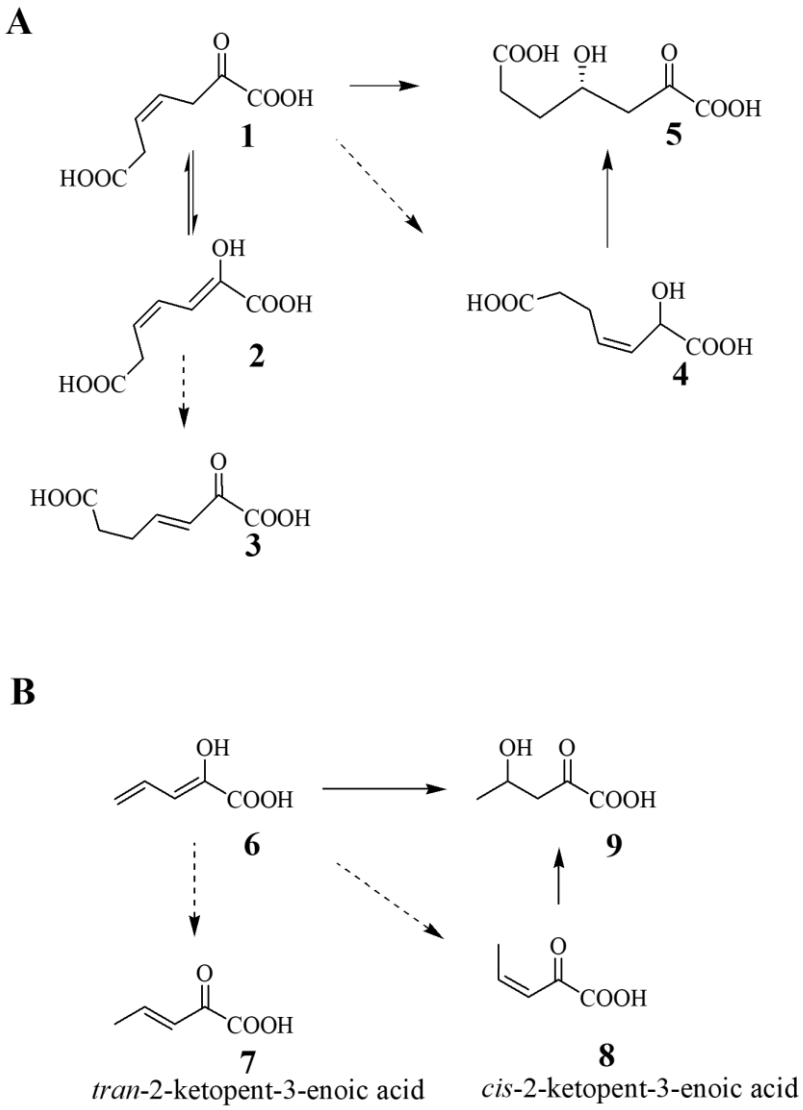

Figure 5. **A**; Reactions of HpcG. HpcG convert 1 and 2 to 5. 1 and 2 are in equilibrium in solution and under a long incubation period, a mixture of 1 and 2 decay to 3 (3E isomer). **B**; Reaction catalyzed by MhpD (Burks et al, 1998; Pollard et al, 1998)

The functional roles of metal in the active sites of different hydratases are different. The crystal structure of HpcG was solved in apo form and with magnesium and oxalate (inhibitor) bound (Izumi et al, 2007). The crystal structure with substrate could not be obtained. The crystal structure contains two pentamers stacked together to form a decamer. In the enzyme active site, magnesium ion is coordinated with Glu106, Glu108 and Glu139 (Figure 6). The oxalate (presumably occupying the substrate position) binds to a magnesium ion. The coordination shell of magnesium ion is almost perfectly octahedral with three residues of glutamate, water molecule and two oxalate

oxygen. Using binding of oxalate as a model to indicate substrate binding, it can predict that the terminal carbonyl group and carbonyl oxygen at C-1 and C-2 atom coordinate the metal ion in a bidentate fashion, favoring the enol tautomer. Asp79 residue forms a hydrogen bond with a water molecule which is in a position close to the C-4 carbon of substrate. However, this water molecule is quite far and might cannot be activated by metal ion during enzyme catalyzed reaction. The metal ion in HpcG seems to be involved with the binding selectivity of substrate enol form rather than directly activating a molecular water (proposed reaction mechanism of HpcG, Figure 7). However, most of this explanation is a proposal that does not have solid data to support. For MhpD, the reaction mechanism was proposed that metal ion involved directly on activation of the attacking water (Pollard, J. R. and Bugg, T. D. H., 1998) similar to GalB (proposed reaction mechanism of GalB, Figure 8) (Mazurkewich, S. et al, 2016). Therefore, the functional roles of metal ion in various hydratases may be different, depending on the enzyme active site.

Although the reaction mechanism of a few hydratases in HPA degradation and related pathway has been studied, several major questions related to the reaction mechanism are still unclear. It is not known how the attacking water molecule is activated in the enzyme active site. What are active site residues or intermediates involved in the reactions? Therefore, more studies on hydratases related to HPA degradation are needed in order to understand the reaction mechanism of this enzyme. Knowledge gained from the mechanistic studies will be useful for future enzyme engineering to control efficiency and specificity of the enzyme.

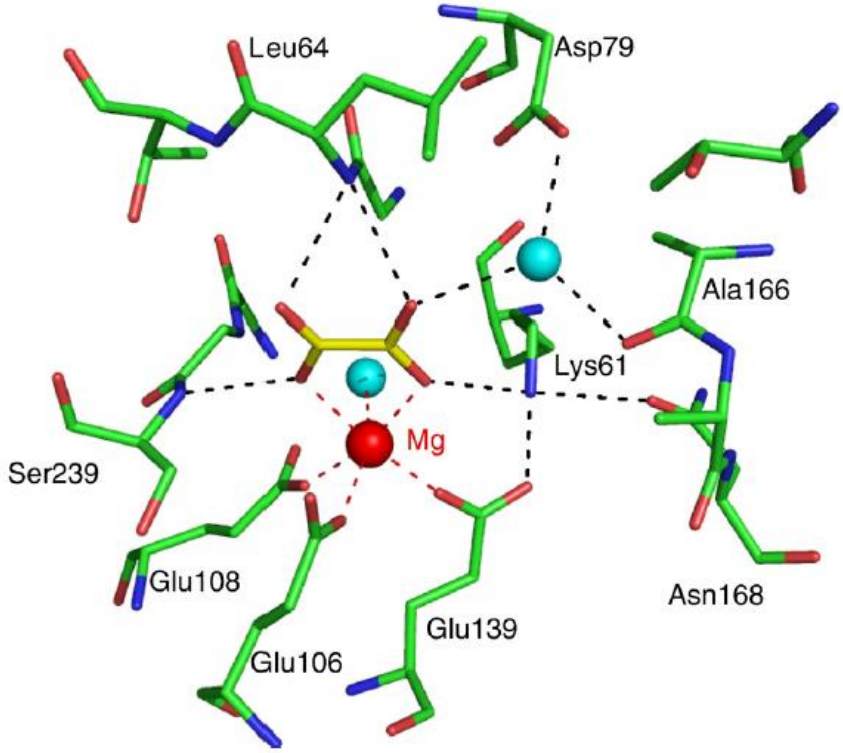

Figure 6. The active site of HpcG with magnesium ion and oxalate bound. Water molecule and magnesium ion are shown in blue and red sphere, respectively (Izumi. A. et al, 2007).

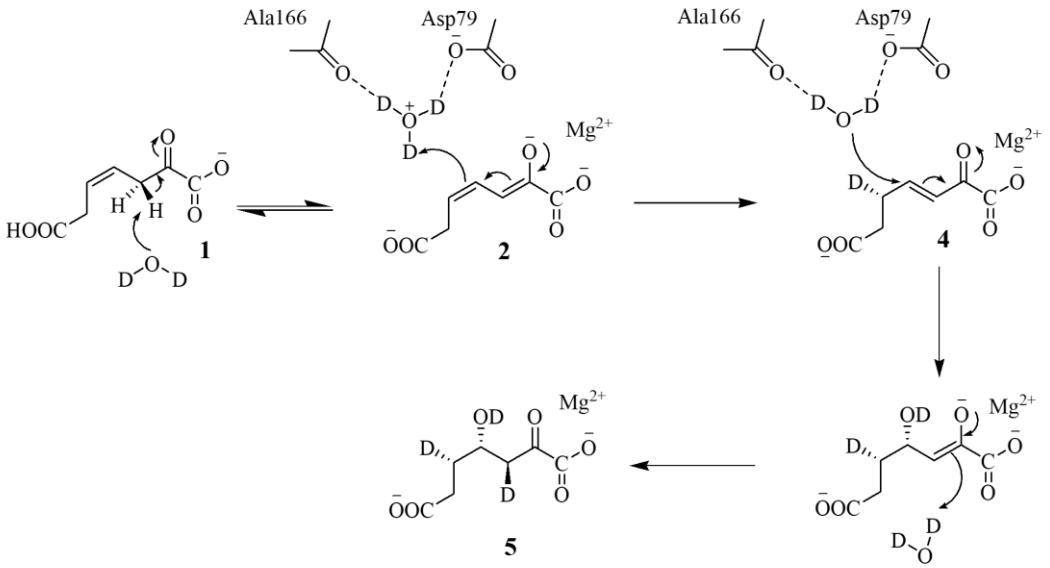

Figure 7. Proposed reaction mechanism of HpcG in D_2O (Adapted from Izumi et al, 2007). Magnesium ion is not directly involved with the activation of water molecule but the water molecule is activated by Asp79.

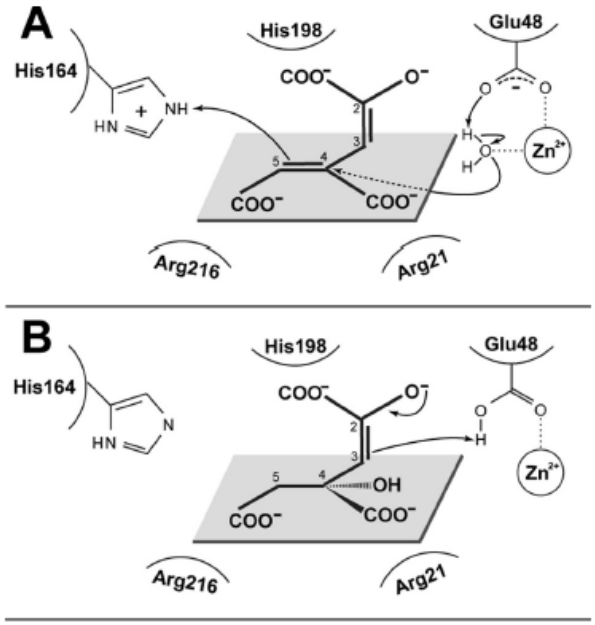

Figure 8. Proposed reaction mechanism of GalB (Mazurkewich, S. et al, 2016). Zinc ion is involved with the activation of a water molecule leading to the addition of the activated water to C4 double bond.

```
OHED_hydra      1 MLDKAKIQELAIQLDEAEKTGQQIRQFSLQYPEITIDDAYAIQKAWVEHKIAEGRKLVGH
HpcG_hydra      1 MFDKHTHTLIAQRLDQAEKQREQIRAISLDYPEITIEDAYAVQREWVRLKIAEGRTLKGH
                  * **       *  ** ***   ***  ** ****** **** *  **  ****** * **

OHED_hydra     61 KIGLTSRAMQVSSNITEPDYGALLDDMVFEEGSDIPMSRFIVPRVEVELAFILDKPLSGP
HpcG_hydra     61 KIGLTSKAMQASSQISEPDYGALLDDMFFHDGSDIPTDRFIVPRIEVELAFVLAKPLRGP
                  ****** *** ** * ********** *  *****  ****** ****** * *** **

OHED_hydra    121 NCTIFDVLDATRYVIPTIEIIDARLHNVDPETQITRKVFDTISDNAANAGIVMGGRPIKP
HpcG_hydra    121 NCTLFDVYNATDYVIPALELIDARCHNIDPETQRPRKVFDTISDNAANAGVILGGRPIKP
                  *** ***  ** **** * **** ** *****  ***************   *******

OHED_hydra    181 NDLDLRRVSAVLYRNGVIEESGVAAAVLNHPAKGVAWLANKLHPHGVTLQPGQIILGGSF
HpcG_hydra    181 DELDLRWISALMYRNGVIEETGVAAGVLNHPANGVAWLANKLAPYDVQLEAGQIILGGSF
                    ****  **  ******** **** ****** ********* *  * *  *********

OHED_hydra    241 TRPVAARAGDTFHIDYDQLGSIAFRFV
HpcG_hydra    241 TRPVPARKGDTFHVDYGNMGSISCRFV
                  **** ** ***** **   ***  ***
```

Figure 9. Amino acid sequence alignment of OHED hydratase and HpcG was analyzed using Blast program in the NCBI database.

The gene encoding for a hydratase in the HPA degrading operon was identified. The enzyme is a probable a 2-oxo-hepta-3-ene-1,7-dioic acid (OHED) hydratase which may catalyze the addition of water into 2-oxo-hept-3-ene-1,7-dioic acid (OHED) and form 2,4-dihydroxy-hept-2-ene-1,7- dioic acid (HHED) (Figure1) (Thotsaporn, K. et al, 2016). Sequence analysis showed that the putative OHED hydratase from *Acinetobacter baumannii* and *E. coli* HpcG have 69% identity and 80% similarity (Figure 9). Therefore, the OHED hydratase in *Acinetobacter baumannii* may catalyze reaction with similar mechanism but may have substrate specificity different from the hydratase from *E. coli*. In this proposal, we propose to characterize biochemical properties of OHED hydratase from the HPA degradation pathway of *Acinetobacter baumannii* and investigate the enzyme substrate specificity. The reaction mechanism of OHED hydratase will also be investigated using steady-state and pre-steady state kinetics and isotope labeling. We will also investigate amino acid residues that may be important for activating H_2O molecule and act as general acid or base.

2.3 Objectives

- To investigate biochemical and biophysical properties of OHED hydratase from *Acinetobacter baumannii*
- To investigate substrate specificity of OHED hydratase
- To elucidate the reaction mechanism of OHED hydratase using pre-steady state and steady-state kinetics and isotope labeling study.
- To investigate amino acid residues that may be important for activating a H_2O molecule in the reaction catalyzed by OHED hydratase

2.4 Research methodology

Plasmid construction, overexpression and purification of OHED hydratase

A putative gene of OHED hydratase will be constructed and cloned into an appropriate expression vector, overexpressed in *E. coli* BL21(DE3) and cultured in an appropriate medium to produce a recombinant OHED hydratase. OHED hydratase will be purified using ammonium sulfate fractionation and various chromatographic methods such as DEAE Sepharose (anion exchange chromatography), Phenyl Sepharose (hydrophobic chromatography) to obtain the purified protein.

Determination of protein concentration, purity and molecular mass

Concentrations of proteins will be determined by the Bradford assay (Bradford, M. M., 1976). The purity of purified enzyme will be determined using SDS-PAGE analysis and stained with Coomassie Blue. The molecular weight of OHED hydratase will be determined by gel filtration FPLC. A standard curve based on mobility of various standard proteins such as b-amylase (molecular mass = 200.0 kDa), alcohol dehydrogenase (molecular mass = 150.0 kDa), bovine serum albumin (molecular mass = 66.0 kDa), carbonic anhydrase (molecular mass = 29.0 kDa), and cytochrome c (molecular mass = 12.4 kDa) will be constructed.

Investigation of substrate specificity of OHED hydratase and product analysis

2-oxo-hept-3-ene-1,7-dioic acid derivatives and various alpha, beta-unsaturated carbonyl will be tested if they are substrates for the OHED hydratase. The purified products will be analyzed by HPLC-MS and NMR spectroscopy.

Kinetic assay and substrate specificity determination

Enzyme assays will be performed in both direct and coupled assays. In direct assays, the OHED hydratase will be assayed according to the previous protocol (Harayama et al., 1989). 2-oxo-hept-3-ene-1,7-dioic acid (OHED) (keton form) and 2-hydroxyhept-2,4-diene-1,7-dioic acid (HHDD) (enol form) will be synthesized according to protocol of (Harayama et al., 1989) and used as substrates of OHED hydratase. The reaction will be followed the consumption of substrates using absorbance at 276 nm (Burks et al., 1998). The coupled assay can be carried out by coupling with the Hpcl aldolase, the next enzyme of the pathway, and lactate dehydrogenae (LDH). The reaction can be followed by monitoring NADH consumption at 340 nm as pyruvate is converted to lactate by LDH. The concentration of substrates will be varied to determine K_m and V_{max}. The data will be analyzed according to a Michaelis-Menten equation by nonlinear regression.

Kinetics of the OHED hydratase will also be investigated using rapid-quench techniques to identify rate constants associated with a first turnover of the reaction. This experiment can identify if the reaction has burst kinetic characteristics. Burst kinetics is consistent with the product release is the rate-limiting step of the reaction.

pH/rate profile and effect of temperature on the reaction of OHED hydratase

Buffers with the same ionic strength within a certain range of pH will be prepared. OHED hydratase will be assayed in the relevant buffer using the previously described. The effect of temperature on the reaction catalyzed by OHED hydratase will be determined by measuring activity of OHED hydratase at various temperatures. Specific activities will be plotted *vs* temperature and analyzed according to the Arrhenius equation.

OHED hydratase metal analysis

In order to determine the metal ions required for catalysis, metal will be removed from the purified enzyme using EDTA and then dialyzed against an appropriate buffer solution to remove EDTA. An apo-enzyme will be assayed in the presence of various divalent metal ions to identify which ion gives a maximum activity.

In order to identify metal ions bound to the native OHED hydratase, the purified enzyme will be analyzed using an inductively coupled plasma mass spectrometry (ICP-MS) and atomic absorption spectroscopy.

Isotope labeling study

The reaction of OHED hydratase using a native substrate (2-oxo-hept-3-ene-1,7-dioic acid) will be carry out in the D_2O buffer. The reaction will be followed by ^{1}H-NMR in order to determine the positions (C3 or C5) of deuterium incorporation into product as described in the previous reports (Burks et al, 1998; Jhonson et al, 2016)

Site-directed mutagenesis

Residues at the active site of OHED hydratase from the HPA degradation pathway of *Acinetobacter baumannii* will be investigated their functions using site-directed mutagenesis studies approach. The OHED hydratase structure will be built based on the 3-D structure of the enzyme homologue from *Escherichia coli* (HpcG) (Izumi, A. et al, 2007) in order to understand the mechanism of reaction catalysis. Site-directed mutagenesis will be performed according to the instruction in the QuickChange® II Site-Directed Mutagenesis Kit manual from Stratagene (La Jolla, CA).

3. Results and discussion

3.1 Expression and purification of OHED hydratase from Acinetobacter baumannii

Expression of OHED hydratase

OHED hydratase was successfully constructed to pET11a recombinant plasmid. The hydratase gene was tried expression in *E. coli* BL21(DE3) using auto–induction media (ZYM). **Figure 3.1** show SDS-PAGE analysis of hydratase expression and the results show that hydratase genes is well expression in soluble form with the molecular weight about 29 kDa which is correlated with the molecular weight calculated from amino acid sequence using ExPASy: SIB Bioinformatics Resource Portal. The expression condition at 25°C for 18 hrs gave the highest amount of OHED hydratase, so this condition was used for large scale overexpression.

Purification of OHED hydratase

Frozen cell paste from the large scale overexpression was thawed and resuspended in a lysis buffer containing 50 mM HEPES pH 7.0, 5 mM EDTA, 1 mM DTT, and 100 µM PMSF. Cells were then disrupted by using sonicator and the suspension after sonication was defined as whole-cell suspension. After that the suspension was centrifuged at 17,000 rpm at 4 ^{0}C for 1 hour, the pellet was discarded. The supernatant was defined as the crude extract. Nucleic acid material from the crude extract was removed by adding 12%v/v of poly(ethyleneimine) to a final concentration of 0.1%(v/v) of crude extract. The cell suspension was centrifuged at 15,000 rpm at 4 ^{0}C for 30 minutes and the pellet was discarded. OHED hydratase was fractionated by ammonium sulphate at final concentration around 10%-30% (w/v) which was resuspended and dialyzed in 50 mM HEPES pH 7.0 for overnight. After that the sampled was loaded in DEAE-Sepharose column which equilibrated with 50 mM HEPES pH 7.0 contained 100 mM NaCl. The column then was washed with 1 liter of 50 mM HEPES pH 7.0 contained 100 mM NaCl to remove impure protein. The OHED hydratase was eluted out using the gradients of NaCl from 100 to 300 mM in 50 mM HEPES pH 7.0. The fractions containing OHED hydratase were pooled, concentrated, and loaded onto a G-25 gel filtration column to remove high salt concentration and exchange buffer to 50 mM HEPES pH 7.0. The SDS-PAGE analysis (**Figure 3.2**) showed that the targeted protein with molecular mass of about 29.7 kDa has high purity (more than 90% purity) after purification and the purified OHED hydratase was obtained about 1 g from 4 liters of cell culture.

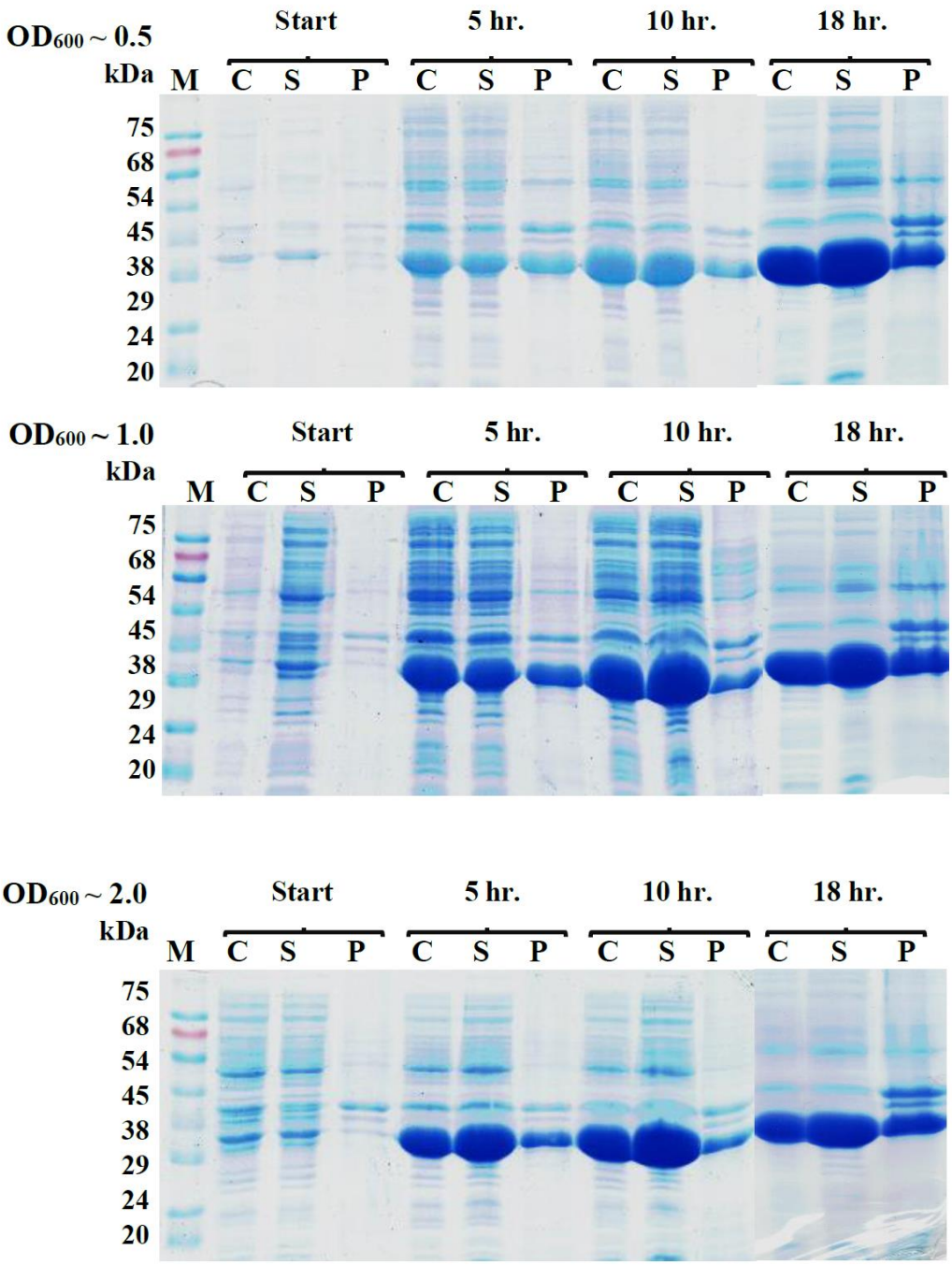

Figure 3.1 SDS-PAGE analysis of OHED hydratase expression in E. coli strain BL21(DE3) in auto-induction media at 25˚C. Cells harboring OHED hydratase were grown at 37˚C and the incubation temperature was changed to be 25 ˚C when OD600 of the culture reached 0.5, 1.0 and 2.0, respectively. The protein expression was allowed to continue for another 18 hr. The samples of culture bacteria of each conditions were collected after induction at various times including 5 hr., 10 hr. and 18 hr., respectively. The cells were harvested and disrupted by sonication in 50 mM HEPES pH 7.0 containing 60 μM PMSF. The crude extract, supernatant and pellet were quantitated using Bradford method and 20 μg of protein of each samples was analyzed using SDS-PAGE (15%) analysis. **Lane M**; protein markers, **Lane C**; crude extract harboring OHED hydratase, **Lane S**; supernatant of induced E. coli harboring OHED hydratase, **Lane P**; pellet of induced E. coli harboring OHED hydratase.

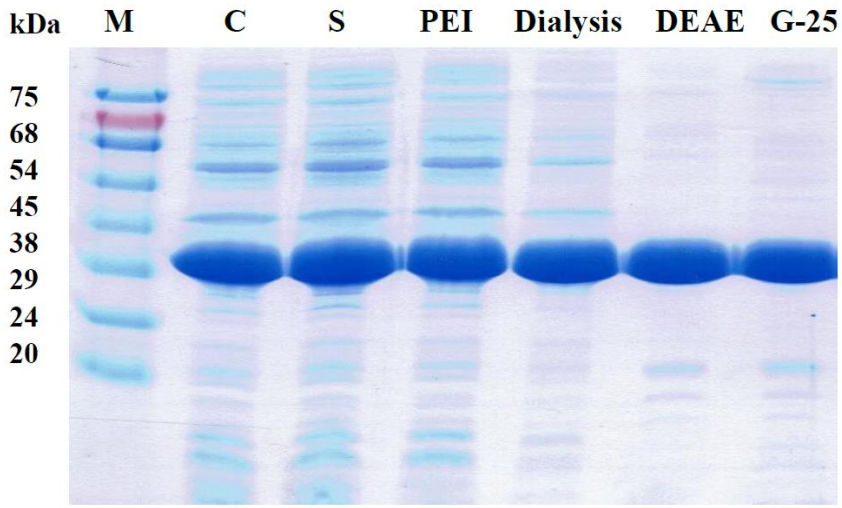

Figure 3.2 SDS-PAGE analysis of OHED hydratase. The sample from each purification step was analyzed by 15% SDS-PAGE. Lane M; standard protein markers, Lane C; crude extract harboring OHED hydratase, Lane S; supernatant of induced E. coli harboring OHED hydratase, Lane PEI; supernatant of induced E. coli harboring OHED hydratase was discarded nucleic acid by 0.1% PEI precipitation, Lane D ; protein solution after dialysis of ammonium sulphate fractionation at final concentration around 10-30% w/v , Lane DEAE; eluting fractions that contain OHED hydratase from DEAE-Sepharose were pooled and concentrated. Lane G-25; protein after desalted, exchanged buffer and concentrated.

3.2 Native molecular mass of OHED hydratase from *Acinetobacter baumannii*

The native molecular mass of OHED hydratase was determined using a Fast Protein Liquid Chromatography (FPLC) (ÄKTA purifier, Bio-Rad, USA) instrument equipped with SephadexTM 200 Increase 10/300 GL size exclusion chromatography column. The commercial proteins that known accurate molecular mass including blue dextran (2000 kDa, V0), thyroglobulin (690 kDa), ferritin (440 kDa), β-amylase (200 kDa), aldolase (158 kDa), bovine serum albumin (66 kDa), ovalbumin (43 kDa), carbonic anhydrase (26 kDa) were used as molecular mass standards. All of protein standards were injected and eluted from a column as showed gel filtration chromatogram in **figure 3.3 A**. The calculating of ratio between elution volume (Ve) and void volume (V0) as a blue dextran to obtain linear equation which derived from the relations of log MW and Ve/V0 (**Figure 3.3 B**) OHED hydratase showed the elution

volume (Ve) at 11.0475 ml so then the native molecular mass of enzyme was calculated to be 300.9805 kDa. The denatural formation of OHED hydratase was analyzed by SDS-PAGE and provided enzyme subunit that is around 29 kDa. Based on the ExPaSy primary structure analysis algorithm indicated molecular subunit of OHED hydratase is 29.7 kDa. Thus, the result represents that the native quaternary structure of OHED hydratase is decameric enzyme. The oligomeric states of OHED hydratase at various forms including holo-OHED, apo-OHED and metal (Mn^{2+}, Zn^{2+}, Ca^{2+} and Mg^{2+}) substitution of apo-OHED hydratase were determined to observe the effect of metal ions on the oligomeric state of OHED hydratase. The results show that all conditions show the same elution volume so the results indicated that metal ions don't involve in oligomer formation of OHED hydratase.

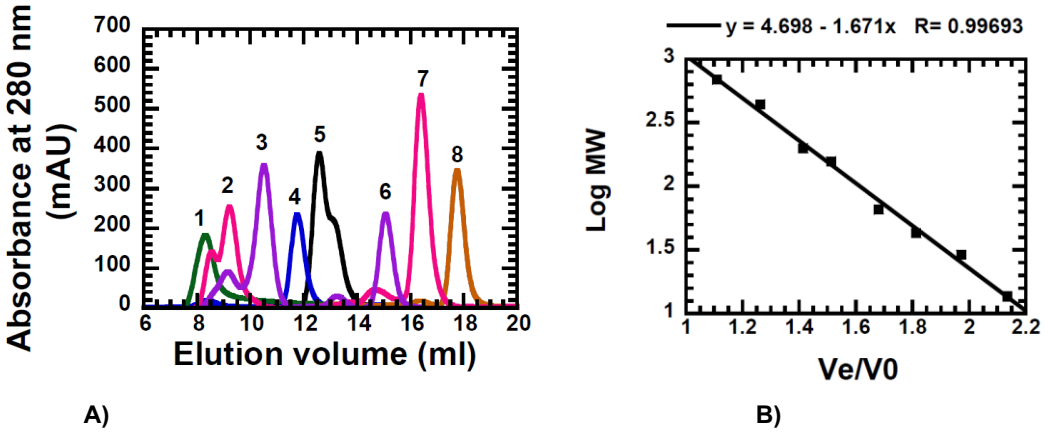

Figure 3.3. A) Gel filtration chromatogram of protein standards and OHED hydratase to determine native molecular weight of hydratrase using SephadexTM 200 Increase 10/300 GL size exclusion chromatography column and elution volume (ml) of the all proteins was showed as 1, 2, 3, 4, 5, 6, 7 and 8 for Blue dextran (2000 kDa), Thyroglobulin (960 kDa), Ferritin (440 kDa), β-amylase (200 kDa), aldolase (158 kDa), bovine serum albumin (66 kDa), Ovalbumin (43 kDa) and carbonic anhydrase (26 kDa), respectively. **B)** The plot of log MW vs Ve/V0 resulting a linear relationship and native molecular weight of OHED hydratase was determined as 300.9805 kDa.

3.3 Native metal identification of OHED hydratase from *Acinetobacter baumannii*

Screening for metal cofactor candidates of OHED hydratase was determined using Microwave Plasma – Atomic Emission Spectrometer (MP-AES) and observation of metal content of metal substituted in Apo-OHED hydratase was performed using Inductive Couple Plasma – Optical Emission Spectrometer (ICP-OES).

Screening of metal cofactor candidates by Microwave Plasma - Atomic Emission Spectrometer (MP-AES)

The MP-AES analysis was calibrated with various concentration of standard metal solutions including Mn^{2+}, Zn^{2+}, Ca^{2+}, Mg^{2+}, Cr^{2+}, Co^{2+}, Ni^{2+} and Cu^{2+}. The standard calibration curve showed linear relationship between emission intensity of metal ion concentration (ppm) in the range of 0-2 ppm (**Figure 3.4**). The purified OHED hydratase was analyzed in the same condition and the concentration of metal candidates that found in enzyme solution was determined (**figure 3.5A**). The result showed that the metal cofactor candidates were Ag^{+}, Al^{3+}, Ba^{2+}, Ca^{2+}, Co^{2+}, Cu^{2+}, Mg^{2+}, Mn^{2+}, Ni^{2+}, Pb^{2+} and Zn^{2+}. The metal contents in the enzyme that purified in different buffering systems, 50 mM of HEPES buffer pH 7.0 and 50 mM of sodium phosphate buffer pH 7.0 were also determined. The results in **Figure 3.5 A** showed that the enzyme that purified using 50 mM of HEPES buffer pH 7.0 has high concentration of metal ions than that using 50 mM of sodium phosphate buffer pH 7.0. It indicated that sodium phosphate buffer act as chelating agent. From this result, 50 mM of HEPES buffer pH 7.0 was chosen as buffer solution in the purification process of OHED hydratase.

The concentration of metal candidate was calculated in term of mole ratio per enzyme subunit to indicate the amount of metal atom occupying in one subunit of the enzyme as shown in **Figure 3.5B**. The results showed that in purified-OHED hydratase had high metal mole ratio of Ca^{2+}, Mg^{2+}, Zn^{2+} and Mn^{2+}. So, these four metal ions were chosen to investigate further using Inductive Couple Plasma-Optical Emission Spectrometer (ICP-OES) analysis.

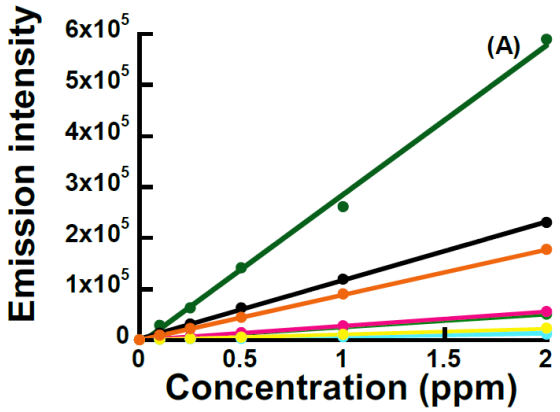

Figure 3.4. Standard calibration curve of various metal ions including Mn (green), Zn (blue), Ca (tight green), Mg (black), Cr (pink), Co (light blue), Ni (yellow) and Cu (orange) in linearity range 0-2 ppm.

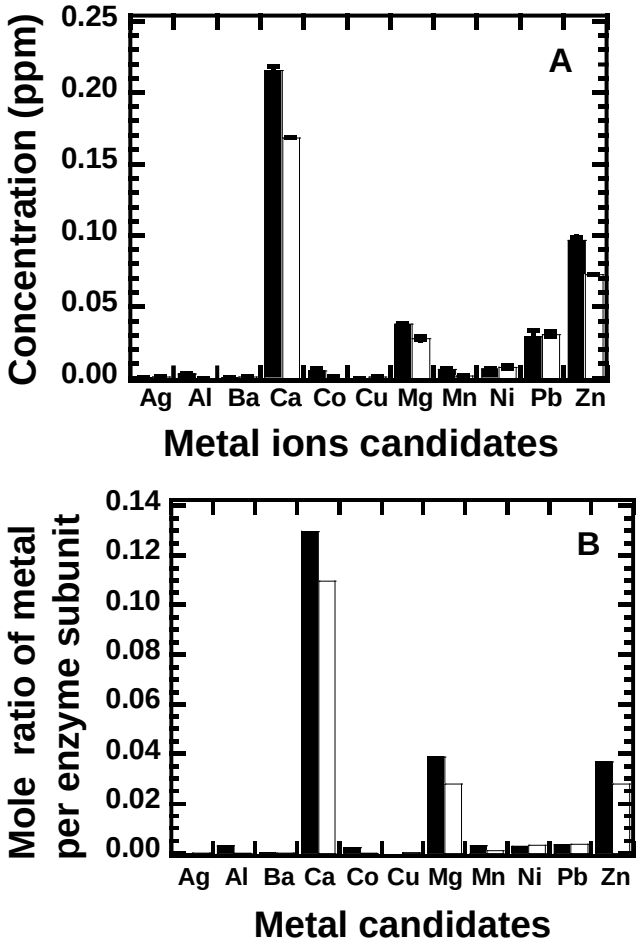

Figure 3.5 Metal candidates of purified hydratase. **A:** Concentration of metal candidates (Ag^{+}, Al^{3+}, Ba^{2+}, Ca^{2+}, Co^{2+}, Cu^{2+}, Mg^{2+}, Mn^{2+}, Ni^{2+}, Pb^{2+} and Zn^{2+}) found in purified-OHED hydratase. **B:** The mole ratio of metal candidates per enzyme subunit is reported. Black and white bars indicate the enzyme purified using 50 mM HEPES pH 7.0, and 50 mM NaH2PO4 pH 7.0 respectively.

Metal content determination in OHED hydratase using Inductive Couple Plasma - Optical Emission Spectrometer (ICP-OES)

Based on MP-OES results, all metal candidates (Mn^{2+}, Zn^{2+}, Ca^{2+}, Mg^{2+} and mixed metal ions) were reconstituted with Apo-OHED hydratase and the amount of metal ions containing in metals substituted enzyme and apo-enzyme were determined and compared using ICP-OES. The experiment using ICP-OES was calibrated with various concentration of standard metals (Mn^{2+}, Zn^{2+}, Ca^{2+} and Mg^{2+}) and the standard calibration curve showed linear relationship between emission intensity and concentration of metal ion in the range of 0-4 ppm. The metal removal efficiency of Apo-enzyme preparation between using EDTA chelating and CHELAX100 resin method were compared as showed in **Figure 3.6 A**. The results showed that preparing Apo-enzyme using CHELAX100 resin is more efficiency than that using EDTA chelating. So Chelex@100 resin was used for the apo-enzyme preparation.

The apo-OHED was substituted with metal candidates including $CaCl_2$, $MgCl_2$, $MnCl_2$, $ZnCl_2$ and mixed metal ions were determined metal content and calculated mole ratio of metal per enzyme subunit. The results in **Figure 3.6 B** showed that the mole ratio of metal ions per enzyme subunit of all conditions was similar which are 1.00, 1.25, 1.30 and 1.24 for Ca^{2+}, Mg^{2+}, Mn^{2+} and Zn^{2+} respectively. However, apo-enzyme reconstituted with mixed metal ions showed the mole ratio of metal ions per enzyme subunit about 0.5 for Zn^{2+} and Mn^{2+}, which higher than Ca^{2+} and Mg^{2+} about 0.2. The results indicated that Zn^{2+} and Mn^{2+} could occupy to enzyme better than Ca^{2+} and Mg^{2+} and it also indicated that Zn^{2+} and/or Mn^{2+} may be a native metal ion for OHED hydratase. We further determined the binding affinity of apo-OHED with Mn^{2+} and Zn^{2+} ions using ITC. Unfortunately, the ITC experiment could not provide any interpretable result.

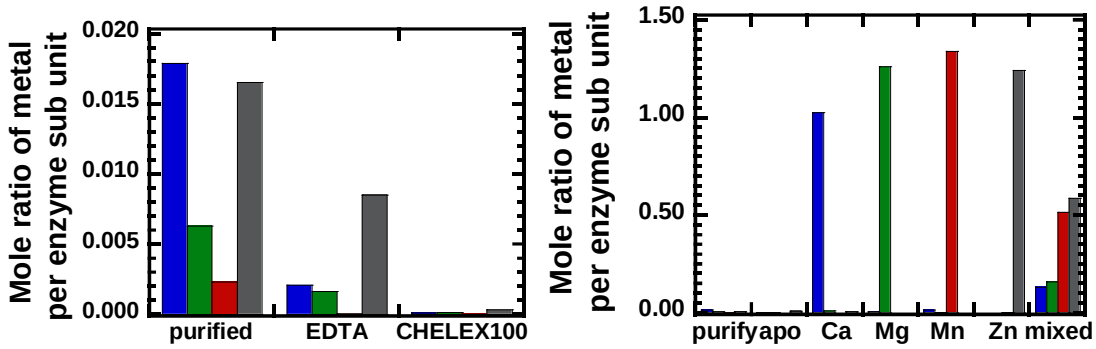

Figure 3.6. (**A)** The efficiency of apo-enzyme preparation between EDTA chelating and CHELAX100 resin were determined with ICP-OES. **(B)** Mole ratio of metal per enzyme sub unit of Apo OHED hydratase substituted with metal candidates; Ca^{2+} (blue), Mg^{2+} (green), Mn^{2+}(red) and Mg^{2+}(gray).

3.4 Effect of pH on the reaction of OHED hydratase

Single component buffer

The activity of purified OHED hydratase was performed at various pHs (pH 3-10) to determine an optimal pH for OHED hydratase activity using single component buffer solution including 100 mM glycine buffer (pH 2-4), 100mM acetate buffer (pH 4-6.5), 100 mM and 100 mM HEPES (pH 7-9). The reaction mixture was initiated by adding OHED hydratase and monitored the product formation using HPLC/MS analysis. The specific activity was calculated and plotted against pH as pH profile activity (**Figure 3.7**). The result showed that the optimal pH for OHED activity is pH 7.0.

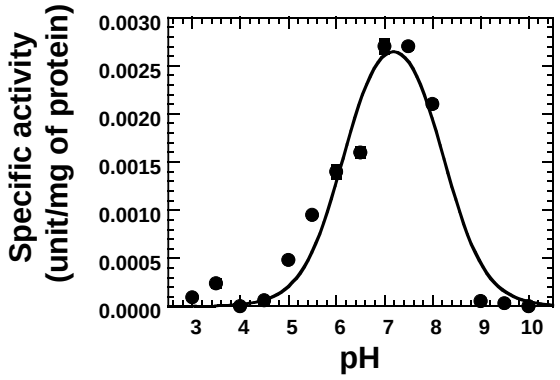

Figure 3.7. The pH dependent activity of OHED hydratase using trans-fumarate as a substrate analogue. The single component buffer system with various pHs from 3 to 10 which are composed of 100 mM of glycine, 100 mM of acetate buffer and 100 mM of HEPES. The OHED hydratase activity were performed with this buffer system. The malate production was determined using HPLC/MS and calculated the specific activity (unit/ mg of protein)

Three component buffer

- *Bis-tris, triethanolamine and acetic acid system*

The activity of purified OHED hydratase was performed at various pHs (pH 4-9) to determine an optimal pH for OHED hydratase activity using three component buffer solution. The buffer at various pHs (pH 4-9) were prepared from three component of 0.05 M Bis-tris, 0.05 M triethanolamine and 0.1 M acetic acid. The reactions were performed by premix solution of trans-fumarate and buffers and the reaction initiated by adding OHED hydratase and the product formation was determined by using HPLC/MS analysis. The pH profile activity of OHED hydratase showed in **Figure 3.8 (A)** and the optimal pH value for OHED activity is 6.4. However, the specific activity of OHED hydratase in the three component buffer system is about 3 fold lower than that single component buffer system at pH 7.0. These results suggest that a component in three component buffer systems may inhibit OHED hydratase activity.

- *MES, diethanolamine and TAPSO system*

The activity of purified OHED hydratase also was performed at various pHs (pH 6-9) to determine an optimal pH for OHED hydratase activity using three component buffer solution of 0.052M 22-(N-Morpholino) ethanesulfonic acid (MES), 0.052M 3-[N-(Trishydroxymethyl)methylamino]-2-hydroxypropanesulfonic acid (TAPSO) and 0.1 M diethanolamine. The pH profile activity of OHED hydratase showed in **Figure 3.8 (B)** and the optimal pH value for OHED activity is 6.7. However, the specific activity of OHED hydratase in this three component buffer system is about 6 fold lower than that single component buffer system at pH 7.0. These results suggest that a component in three component buffer using MES, diethanolamine and TAPSO system may inhibit OHED hydratase activity and it also showed strongly inhibit reaction more than three component buffer of bistris, triethanolamine and acetic acid system.

The study of the effect of pH on the reaction of OHED hydratase using trans fumarate as substrate analogue in this section can conclude that the optimal pH for OHED hydratase is pH 7.0. Using three component buffer of Bis-tris, triethanolamine and acetic acid system and MES, diethanolamine and TAPSO system inhibit the activity of OHED hydratase. So 100 mM HEPES buffer pH 7.0 is the suitable buffer for OHED hydratase assay.

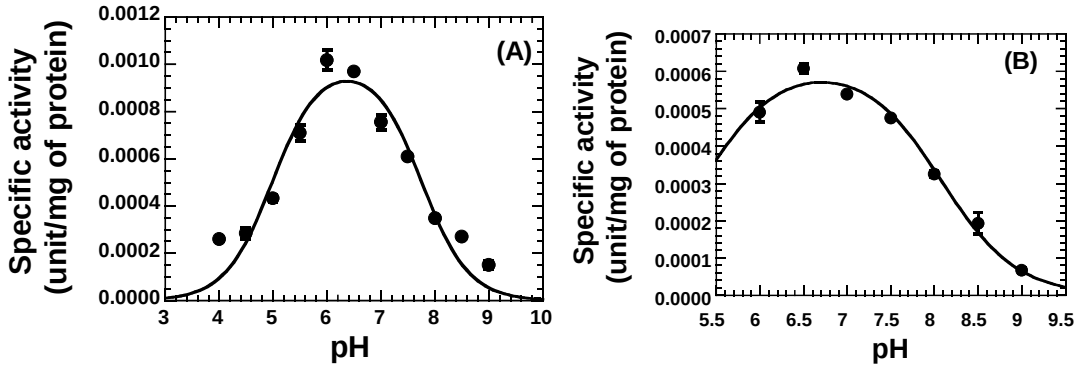

Figure 3.8 The pH dependent activity of OHED hydratase using trans-fumarate as a substrate analogue. **A)** pH dependent activity of OHED hydratase in bis-tris, triethanolamine and acetic acid buffering system. **B)** pH dependent activity of OHED hydratase in MES, diethanolamine and TAPSO buffering system

4.5 The effect of temperature to the OHED hydratase activity

The activity of OHED hydratase using trans-fumarate substrate was determined in 100 mM HEPES, pH 7.0 at various temperatures (5˚C-70˚C). The reaction mixture was performed by premixing of trans-fumarate in 100 mM HEPES, pH 7.0 at room temperature and then aliquot into 1.5 ml microcentrifuge tube and incubated at 5˚C-70˚C for 15 min. The reaction was initiated by adding OHED hydratase and the reaction mixture was incubated for 30 min and quenched with 5% of formic acid. The product formation was determined using HPLC/MS and the specific activities (unit/mg of protein) was calculated and the activity–temperature profile was plotted as shown in **Figure3.9**. The results indicated that the optimal temperature for the activity of the enzyme was 40˚C.

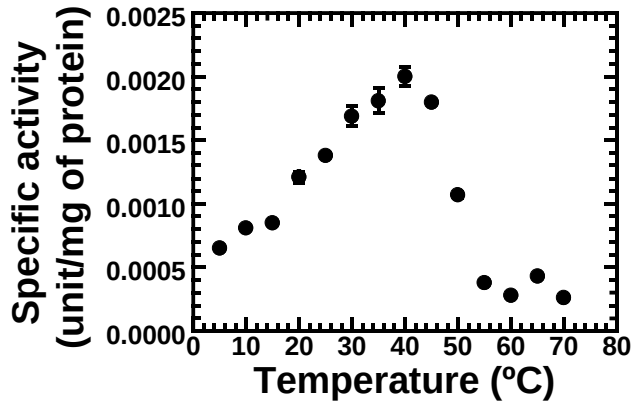

Figure 3.9 The activity – temperature profiles of OHED hydratase with transfumarate substrate. The specificity of OHED hydratase at various temperatures (5˚C-70˚C) were determined and plotted against temperature.

3.6 Thermostability of OHED hydratase in the presence of various metal ion

The effect of metal ion on structural stability of OHED hydratase was determined using Thermoflour assay, the temperature was varied in the range of 25˚C-95˚C using RT-PCR program. OHED hydratase of various forms including to purified-enzyme, apo-enzyme, and metal substitution of apo-enzyme were determined and compared the melting temperature (Tm). The melting curve of the first derivative of fluorescent intensity (dRFU/dT) versus temperature (˚C) was used to determined Tm and the lowest value of curve indicated a melting temperature of enzyme. The results showed that the melting temperatures of purified-OHED (light green) and purified-OHED incubated with various metal chloride ions as Co^{2+} (purple), Mn^{2+} (light blue), Zn^{2+} (blue), Ca^{2+} (orange), Mg^{2+} (pink), Cu^{2+} (green), Fe^{2+} (cyan) and Ni^{2+} (green) in were similar with the value of 58˚C, but the Tm of Zn-OHED (blue) showed a lower Tm with the value of 46˚C (**Figure 3.10A**). This result related with Tm of apo-OHED hydratase substituted various metal ions as apo-OHED (purple), Mn-apo-OHED (light blue), Zn-apo-OHED (blue), Ca-apo-OHED (orange), Mg-apo-OHED (pink) and mixed metals substitution of apo-OHED (green) (**Figure 3.10B**), indicating that metal ions did not enhance the enzyme stability since purified-enzyme and apo-enzyme showed the same Tm. Interestingly, in case of Zn-OHED and Zn-apo-OHED, the enzymes showed lower Tm that indicated the destabilizing effect of Zn^{2+} on OHED hydratase. Also the results from apo-OHED substituted with mix metal ions (the mixture of Mn^{2+}, Ca^{2+}, Zn^{2+} and Mg^{2+}) showed similar Tm to Zn-apo-OHED. This may indicate that in the mixture of metal ions, Zn^{2+} is able to bind tighter than others metals. However, it is unclear how the binding of Zn^{2+} decreases the stability of OHED hydratase. The geometry of Zn^{2+} binding to enzyme may be different from the other metal ions. Generally, the coordination of Zn^{2+} with amino acid in enzyme active site is tetrahedral (Laitaoja et al. 2013) but Mn^{2+}, Ca^{2+} and Mg^{2+} are octahedral (Bujacz et al. 1997), so the geometry of the coordination of metal ion with amino acid residues in enzyme active site may affect the enzyme stability.

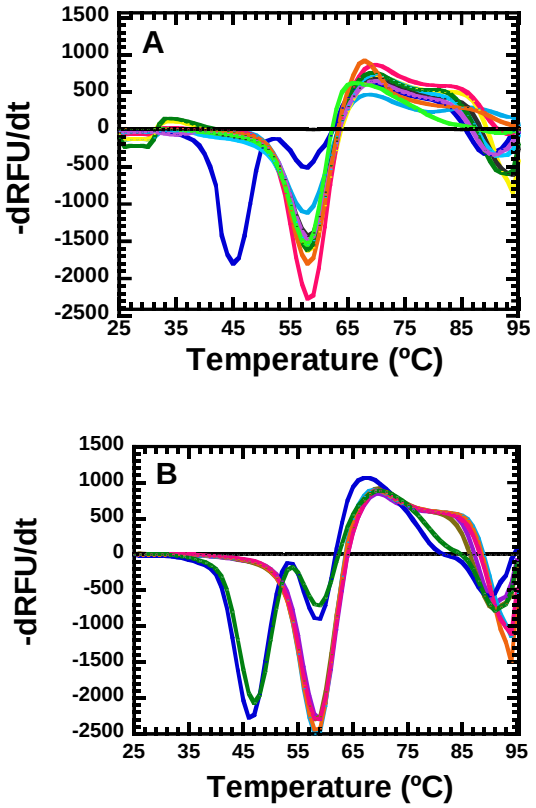

Figure 3.10. The melting curve of OHED hydratase with various metal ions using thermofluor assay. The first derivative curve is plotted between -dRFU/dT of fluorescent intensity and temperature (˚C). The melting temperature (Tm) corresponds to the lowest point of first derivatives (-dRFU/dT). The OHED hydratase with various forms were investigated as Holo-OHED (light green), Apo-OHED (purple), Mn-Apo-OHED (light blue), Zn-Apo-OHED (blue), Ca-Apo-OHED (orange), Mg-Apo-OHED (pink) and mixed metals substitution of Apo-OHED (green).

3.7 Substrate specificity of OHED hydratase from *Acinetobacter baumannii*

The native substrate for OHED hydratase is not commercially available. In order to determine OHED hydratase activity, the substrate screening was performed and focused on the compounds that chemical structure containing of carbon double bond adjacent to carboxyl group (Table 1). The enzymatic reaction was performed with various substrates including cinamic acid, 4-hydroxy cinamic acid (caffeic acid), 3,4-dihydroxy cinamic acid (p-coumaric acid), 3,4,5-trihydroxy cinamic acid (THCA), trans-ferulic acid, crotonic acid, cis –maleic acid, trans-fumaric acid and oleic acid (C18:1) and compared between reaction with (reaction) and without (negative control) enzyme. Among all tested substrates, there was no new product peak observed, except for trans-fumarate and L-malate reaction. These new product peaks were expected to be malate and fumarate, respectively. The results were confirmed by a similar retention times with authentic malate standard.

In cis-maleic acid, which is isomer of trans-fumaric acid, the enzyme cannot catalyze reaction to produce new product. So the result indicated that the OHED hydratase has a regiospecificity. Moreover, we also found that the enzyme cannot catalyze reaction using substrates that structure containing of aromatic ring and/or containing of only one carboxylic group at terminus as cinamic acid, caffeic acid, p-coumaric acid, THCA and trans-ferulic acid. These results indicated that OHED hydratase has very high substrate specificity. So, trans-fumaric acid was chosen as substrate for enzyme assay to study the effect of metal ion on the activity of enzyme.

Table 1. Chemical structures of substrates for screening OHED hydratase activity.

Substrate	Chemical structure		Exact mass (m/z)		New product peak
	substrate	product	substrate	product	
Cinamic acid	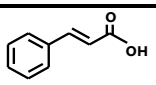	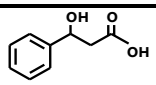	148.05	166.06	X
4-hydroxy cinamic acid (Caffeic acid)	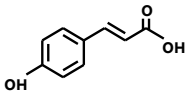	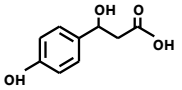	164.05	182.06	X
3,4-dihydroxy cinamic acid (*p*-coumaric acid)	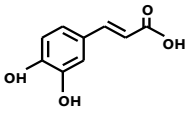	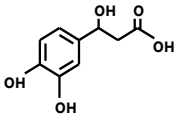	180.04	198.05	X
3,4,5-trihydroxy cinamic acid (THCA)	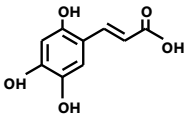	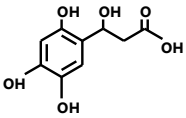	196.04	214.05	X
trans-ferulic acid	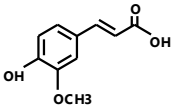	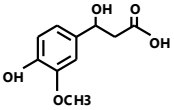	194.06	212.07	X
Crotonic acid	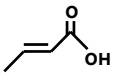	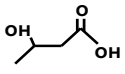	86.04	104.05	X
cis –maleic acid	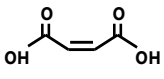	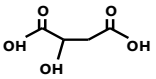	116.01	134.02	X
trans-fumaric acid	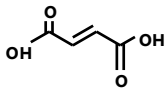	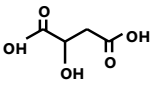	116.01	134.02	√
L-malate	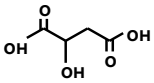	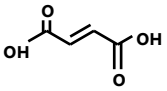	134.02	116.01	√

[a] (√) indicates product formation and (X) indicates no product formation.

[b] All of substrates using in this study can be divided into two groups based on the chemical structure 1) aromatic carbon double bond conjugated carboxyl group and 2) aliphatic carbon double bond conjugated carboxyl group which are consist of cis- or trans- formation.

OHED hydratase substituted with various metal ions (Mn^{2+}, Zn^{2+}, Ca^{2+} and Mg^{2+}) and mixed all metal ions were assayed using trans-fumaric acid as substrate. The specific activity of malate formation of all metal-substituted enzymes were compared and summarized in Table 2. The results showed that the activity of purified OHED, apo-OHED and Mn^{2+}, Ca^{2+} and Mg^{2+}-substituted enzymes are similar. However, the absent of activity found in Zn^{2+}-substituted enzyme and metal mixture-substituted enzymes. The results indicated that the binding of Zn^{2+} ion in active site of the enzyme can inhibit enzyme activity for catalyzing reaction using trans-fumaric acid as substrate. This result correlate with the results of the previous section that Zn^{2+} metal ion can decrease the

enzyme stability. Zn^{2+} has been found to have different chemical co-ordination as represent as tetrahedral fashion and trigonal bipyramid (Mazurkewich et al. 2016) when compared with octahedral fashion for Mn^{2+} and Mg^{2+} (Wang et al. 2005, Fukasawa et al. 2011). In thermophilic nitrile hydratase, Zn^{2+} inhibited the enzyme activity, probably due to their reaction with essential sulfhydryl groups in active site, while magnesium chloride had no effect (Cramp et al.1999). The Zn^{2+} and Mn^{2+} found to have inhibitory effect on δ-aminolevulinic acid dehydratase and phosphopyruvate hydratase activities (Chiba et al. 1984, Saito 1967).

Table 2. The specific activity of OHED hydratase activity with *trans*-fumarate using various metal substitution.

Conditions	**Specific activity** (μ**mole min^{-1} mg protein $^{-1}$**)	**R^2**
Purified-OHED	0.018	0.9929
Apo-OHED	0.015	0.9999
Mn^{2+}-OHED	0.016	0.9981
Zn^{2+}-OHED	0.0000	0.0000
Ca^{2+}-OHED	0.015	0.9972
Mg^{2+}-OHED	0.014	0.9975
Mixed-OHED	0.0000	0.0000

4.8 Steady-state kinetic parameters of reaction catalyzed by OHED hydratase

Steady-state kinetic parameters of OHED hydratase were investigated in 100 mM HEPES pH 7.0 at ambient temperature using trans-fumarate as substrate. The initial velocity of OHED hydratase activity at various concentrations of trans-fumarate (5, 10, 20, 50, 100, 200, 500, 1000 and 2000 μM) was determined using enzyme concentration of 25 μM. The initial velocity of the reaction was calculated from the slope of relative plot between malate formation (μM) and time (min). The kinetic parameters as K_m and V_{max} were obtained from the plot of initial velocity (μM/min) and substrate concentration (μM) according to Michaelis-Menten equation as shown in Figure 3.11A. The K_m and V_{max} were determined to be 1.22 ± 0.07 x 10^{-5} M and 1.27± 0.02 x 10^{-8} M/s, respectively (Table 3).

The steady-state kinetic parameters of reversible activity of OHED hydratase were also determined using similar conditions described in forward reaction, but using L-malate as a substrate. The kinetic parameters (K_m and V_{max}) were obtained from the plotted of initial velocity (μM/min) versus substrate concentration (μM) as shown in Figure 3.11B. From the plot, K_m and V_{max} were determined as 1.29 ± 0.04 x 10^{-4} M and 4.07 ± 0.03 x 10^{-9} M/s, respectively (Table 3). Moreover, the catalytic constant (k_{cat}) was calculated from the maximum velocity divide by total enzyme concentration. The results were summarized in Table 3 and showed that k_{cat} of forward reaction was about 30 folds higher than the k_{cat} of reverse reaction. The catalytic efficiency (k_{cat} /K_m) of forward and reverse reaction were calculated and compared in Table 3. The result showed that OHED hydratase catalyzed hydration 30-time more efficient than those of dehydration reaction.

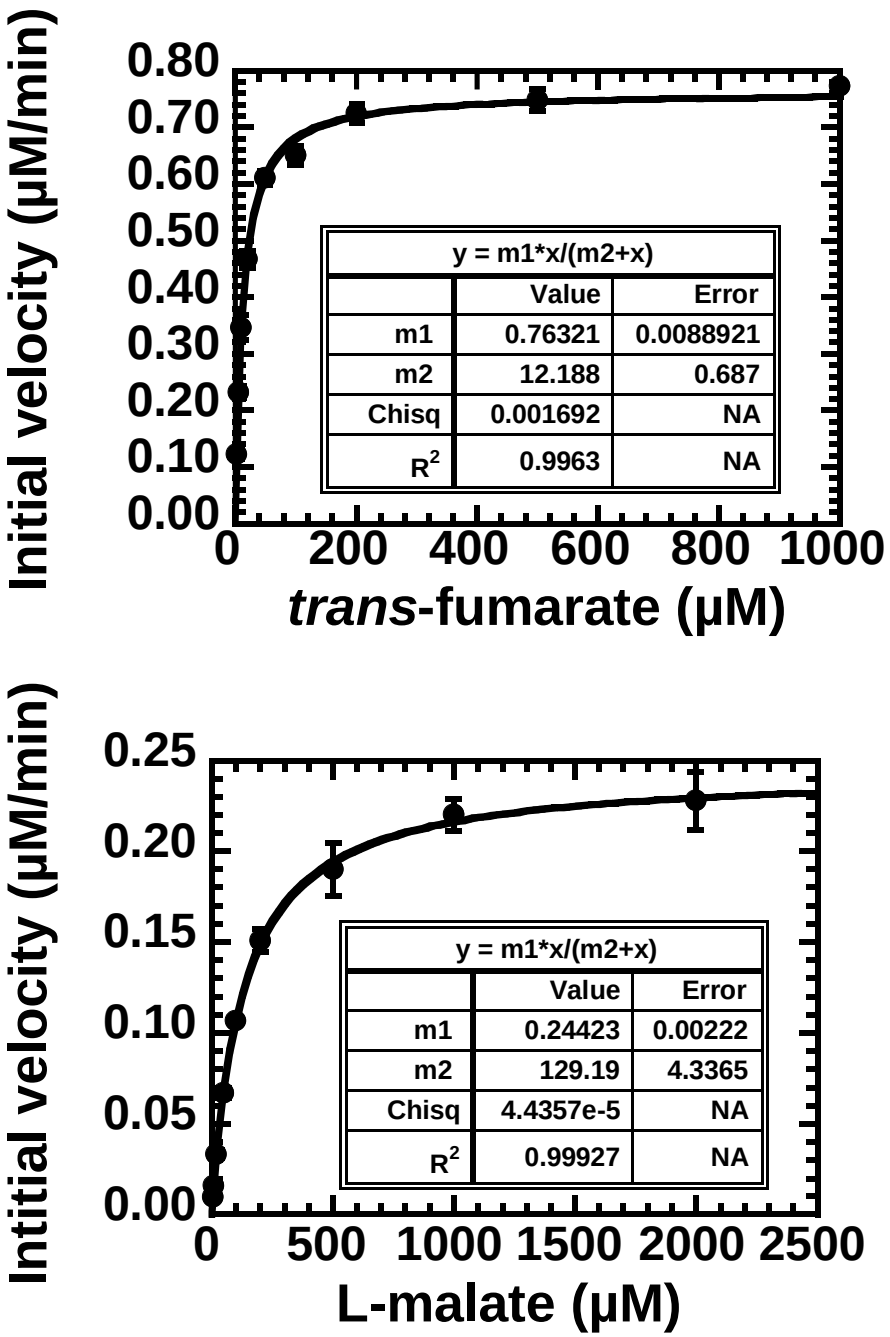

Figure 3.11 Michaelis – Menten plot of forward and reverse reaction catalyzed by OHED hydratase. The kinetic parameters were obtained from the plot of initial velocity (µM/min) versus substrate concentration (µM) according to Michaelis-menten equation. The graphs were plotted and fitted curve in the Michaelis-Menten model by Kaleida Graph program. The plot for the reaction of A) trans-fumarate and B) L-malate.

Table 3. Steady-state kinetic parameter of AbOHED hydratase with hydroxylation and dehydration activity

Kinetic parameter	Forward reaction	Reverse reaction
K_m (M)	$1.22 \pm 0.07 \times 10^{-5}$	$1.29 \pm 0.04 \times 10^{-4}$
v_{max} (M/s)	$1.27 \pm 0.02 \times 10^{-8}$	$4.07 \pm 0.03 \times 10^{-9}$
k_{cat} (s^{-1})	$5.07 \pm 0.07 \times 10^{-4}$	$1.63 \pm 0.02 \times 10^{-4}$
k_{cat}/K_m (M^{-1} s^{-1})	41.5 ± 0.95	1.26 ± 0.38

4.9 Stereo-specificity of OHED hydratase catalyze reverse reaction

From the enzyme activity assay in section 3.7 Substrate specificity investigation of OHED hydratase indicated that the OHED hydratase was specific for trans-fumarate, so substrate stereo-specificity for reverse reaction was investigated by comparing the enzyme activity when substrate either L-malate or racemic mixture of D,L-malate was used. The reaction was performed at low concentration of substrate (5, 10, 15, 20 and 25 μM) and using 25 μM of OHED hydratase. At this condition, the reaction may occur only one round (single turnover reaction) because the concentration of substrate was less than or equal to concentration of enzyme. This experiment might be clarifying the stereo-specific of OHED hydratase. If enzyme has a stereo-specific with L-malate, the specific activity of L-malate condition is higher than the D,L-malate condition around 2 folds. In other hand, if enzyme has stereo-specific with D-malate, the fumarate formation should be found in D,L-malate condition only. While if the enzyme has not stereo-specific, the specific activity of D,L-malate and L-malate condition should be the same value.

The reaction mixture was performed in 100 mM HEPES pH 7 and incubated at room temperature for 3 hr. The reaction was quenched using 5% formic acid and the formation of fumarate was determined using HPLC-MS and the specific activity (unit/mg of protein) was calculated. The results indicated (Figure 3.12) that the fumarate

production of reverse reaction using L-malate substrate was approximately 2 times higher than using racemic D,L-malate substrate. The result clearly indicated that OHED hydratase was specific to L-malate substrate in reverse reaction.

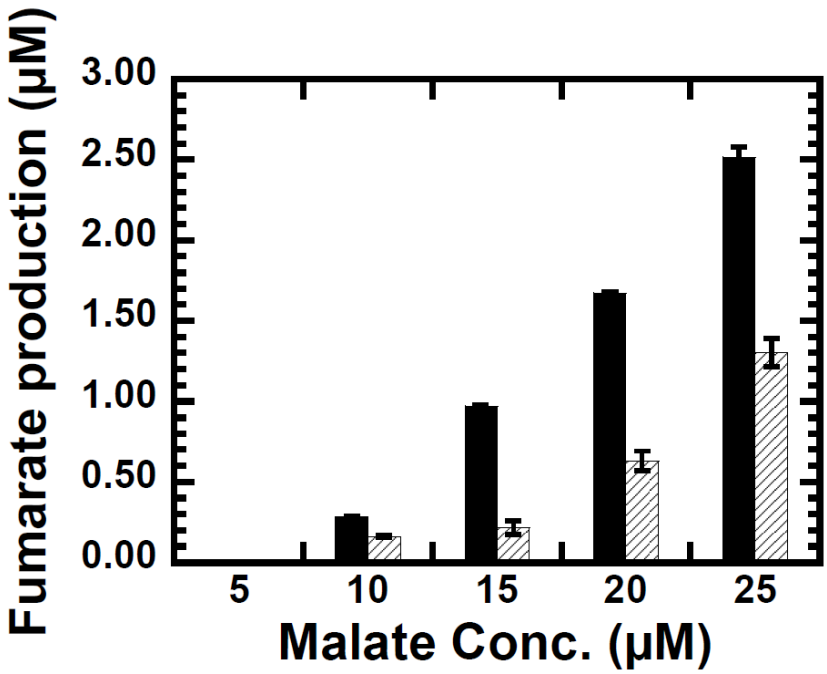

Figure 3.12 Fumarate production of OHED hydratase catalyze reaction using D,Lmalate and L-malate substrate. The reversible reactions were performed in 100 mM HEPES pH 7.0 with various concentrations of L-malate (black bars) and D,L-malate (white bars) for 3 hr at room temperature after adding 25 μM of OHED hydratase.

4. Conclusion and Discussion

2-oxo-hepta-3-ene-1,7-dioic acid (OHED) hydratase catalyzes the water addition to unsaturated carbon bond substrate of 2-oxo-hepta-3-ene-1,7-dioic acid. The new chiral carbon atom of alcohol compound is produced as a 2,4-dihydroxy-hepta-2-ene-1,7-dioic acid. Several hydratases in HPA degradation pathway and related pathway have been studied. It was found that all enzymes were divalent metals-dependent, such as Zn^{2+} cofactor in 4-carboxy-2-hydroxymuconate hydratase, GalB (Mazurkewich et al. 2016) and (3Z)-2-keto-4-carboxy-3-hexenedioleatete, LigJ (Hogancamp 2018), Mg^{2+} cofactor in 2-oxo-hept-4-ene-1,7-dioleatete hydratase, HpcG (Izumi et al. 2007) and 2-hydroxypent-2,4-dienoleatete hydratase, BphH (Wang and Seah 2005), and Mn^{2+}

cofactor in 2-hydroxypentadienoic acid hydratase, MhpD (Adachi et al. 2006) and vinylpyruvate hydratases, VPH (Johnson Stack et. al. 2016). Sequence analysis of deduced amino acid of OHED hydratase from 4-HPA degradation of *A. baumannii* suggested that OHED hydratase may require a metal ion cofactor as it had percent identity up to 72.28% and 32.71% with HpcG in homoprotocatechuate degradation of *E. coli* and MhpD in 3-phenylpropanoleatete degradation of *E. coli*, respectively. Both of HpcG and MhpD are metal-dependent enzymes requiring divalent metals for their activity (Izumi et al. 2007, Adachi et al. 2006). HpcG hydratase, the highest percent identity to OHED hydratase, showed specificity for metal cofactors with more preference toward Mn^{2+} as a native metal cofactor but showed the highest activity with Mg^{2+} (Izumi et al. 2007). This is similar to the MhpD metal-dependent enzyme (Adachi et al. 2006). However, the results of reaction of OHED hydratase with substrate analogue indeed showed metal independent activity, probably suggesting another catalytically function of enzyme in this group if it catalyzes non-natural substrate. In this study, we have studied new OHED hydratase from A. baumannii and reported the biocatalytic properties of the enzyme which is unique and different from the previous report hydratases.

Biochemical and biophysical properties of OHED hydratase

The OHED hydratase was successfully overexpressed in pET11a using auto-induction rich media. This enzyme could be overexpressed in soluble form in *E. coli* system. The highest amount of OHED hydratase could be produced at condition of 25°C for 18 hr. The OHED hydratase was purified with 3 steps of purification process including PEI precipitation, ammonium sulfate precipitation and DEAE column which provided approximately 1 g enzyme from 4 L culture judged to 95% purity (Figure 3.2). The purified OHED was stored in 50 mM HEPES pH 7.0 at -80˚C before using.

The native molecular mass of OHED was determined by gel filtration chromatography using FPLC analysis as 300.9805 kDa (Figure 3.3) while enzyme subunit analyzed by SDS-PAGE was 29.7 kDa. So, this indicated the quaternary structure of decameric enzyme. This is similar to the HpcG in homoprotocatechuate degradation of E. coli that is decameric enzyme (Izumi et al. 2007). The crystal structure of HpcG showed a dimer of pentamer ring stacked together to form decameric structure (Adachi et al. 2006). While MhpD in the degradation pathway of phenylpropionic acid from E. coli has a subunit molecular mass of 28 kDa (Pollard and Timothy 1998) and the crystal structure of MhpD showed the quaternary structure of enzyme is pentameric (Montgomery et al. 2010).

Metal analysis of OHED using MP-AES and ICP-OES techniques indicated that various divalent metals were found in purified enzyme, including Mn^{2+} Zn^{2+} Ca^{2+} and Mg^{2+} (Figure 3.6A). After the apo-enzyme was prepared and substituted with each metal ion candidate, the mole ratio of metal ion per enzyme subunit was not significantly different. However, when the apo-enzyme was substituted with mixed-metal ions, the results showed that mole metal ratio per enzyme subunit of Mn^{2+} and Zn^{2+} were similar (0.5:0.5 mole ratio) and these values were higher than other metal ions, indicating higher occupancy of Mn^{2+} and Zn^{2+} metal ions (Figure 3.6B). When the effect of metal ion on enzyme activity was studied using trans-fumarate as substrate. It was found that purified enzyme, apo form and apo-enzyme substituent with metal candidates had similar enzyme activity. However, no enzyme activity was detected in all conditions containing Zn^{2+} ion. These results well correlate with the thermal stability result using Thermal Shift Assay (ThermoFluor), in which all conditions containing Zn^{2+} ion decreased the melting temperature of enzyme from 58˚C to 46˚C, while other metal ions did not alter the melting temperature of the enzyme.

Therefore, all metal analysis, enzyme activity and thermal shift assay potentially indicate that native metal cofactor of OHED hydratase is likely to be Mn^{2+}, since it can occupy the apo enzyme better than other ions without decrease thermal stability of enzyme.

The functional role of metal ion and water activation on OHED hydratase

The functional roles of metal in the active sites of different hydratases in HPA degradation pathway and related hydratase have been studied. In HpcG, the crystal structure was solved in apo form, with Mg^{2+} and oxalate (inhibitor) bound (Izumi Rea et al. 2007). It revealed that Mg^{2+} ion was coordinated with Glu106, Glu108 and Glu139 and the oxalate binds to a Mg^{2+} ion (Figure 6). Using oxalate binding as a model to indicate substrate binding, it could predict that the terminal carboxyl group and carboxyl oxygen at C-1 and C-2 atom coordinated the metal ion in a bidentate fashion, favoring the enol tautomer. Asp79 residue formed a hydrogen bond with a water molecule which was in a position close to the predicted C-4 carbon of substrate. However, this water molecule was quite far and might not be activated by metal ion during enzyme catalyzed reaction. The enzyme completely lost activity if this aspartate residue was mutated to Alanine (Izumi Rea et al. 2007). The metal ion in HpcG seems to be involved with the binding selectivity of substrate enol from rather than directly activating a molecular water. In LigJ, Glu284 residues was proposed to act as general acid to

abstract proton from water molecule for nucleophilic attack of substrate, while Zn^{2+} is important for substrate binding and facilitate the nucleophilic attack by stabilization of the delocalization of the negative charge via the carbonyl group at C2 of substrate (Hogancamp Mabanglo et al. 2018). For MhpD, the reaction mechanism was proposed that metal ion directly involved on activation of the attacking water (Pollard Bugg 1998) and the enzyme required native metal cofactor for catalytic reaction (Wang and Seah 2005). The functional role of metal ion of MhpD is similar as proposed reaction mechanism of GalB in which Zn^{2+} ion is involved with the activation of a water molecule leading to the addition of the activated water to C4 double bond (Mazurkewich Brott et al. 2016). In BphH, the changing of metal ion cofactor led to alters k_{cat} rather than K_m, suggesting the metal had a catalytic role rather than involved in a substrate-binding (Wang and Seah 2005). Therefore, the functional roles of metal ion in various hydratases were different and depending on the enzyme active site.

In this study, OHED hydratase activity toward trans-fumarate substrate was found to independent on metal ion (table 2). The activation of water molecule in OHED hydratase active site seems to not involved with metal ion. Because the hydration rate of apo-form and metal ion substituent to apo-form showed similar value. This result indicates that the hydration can proceed without the facilitation of metal ions when using trans-fumarate and L-malate as substrate. So the water addition might be activated by amino acid residue residing in enzyme active site. This phenomenon was also previously reported in HpcG, in which water molecule was activated by Asp79 (Izumi Rea et al. 2007). In order to address this notion, the information from site-directed mutagenesis will be further studied. However, in case of native substrates of OHED, the enzyme might strictly require the metal cofactor and we cannot exclude the role of metal in the enzyme catalysis.

The effect of pH and temperature on OHED hydratase activity

pH-dependent profiling based OHED hydratase activity assay using trans-fumarate was carried out in various buffer systems (single component and three-component buffers). In single component buffer, the enzyme showed the highest specific activity in 100 mM HEPES pH 7.0 (Figure 3.7). In order to control an effect of ionic strength, the three-component buffers (bis-tris, triethanolamine, acetic acid and MES, TAPSO, diethanolamine) were used and the enzyme showed the optimal pH in the range of 6-6.5 (Figure 3.8). However, the specific activity of the enzyme in both three-component buffer systems were lower than a single component buffer about 3

folds, indicating that component in buffer may inhibit the reaction of malate production. The optimal pH of OHED hydratase activity is slightly acid and narrower than the other hydratases in aromatic degradation. In BphH, a constant hydration activity was observed at pH values between 6.0-8.0 conducted in constant ionic strength pH buffers. The activity of the enzyme rapidly decreased when the reaction performed out of this pH range (Wang and Seah 2005). This were similar with the MhpD and GalB hydratases which have an optimal pH in the range of 5.5-8.0 and 6.5-8.0, respectively (Wang and Seah 2005, Mazurkewich Brott et al. 2016). The similar of pH optimum range of MhpD and GalB hydratases suggests that both enzymes utilize similar residues with pKa values for catalysis and may be different from the OHED hydratase. Optimum temperature of OHED hydratase was carried out with enzyme activity assay in 5-70˚C conditions. The optimal temperature of OHED hydratase activity was determined as 40˚C (Figure 3.9). The specific activity was rapidly decreased when the temperature was higher than 45˚C and completely lost activity when the temperature was higher than 50˚C. This situation might be the effect of the loss of protein stability and precipitation during temperature increment. The enzyme precipitation was observed when the temperature was increased more than 40˚C.

The substrate specificity and stereo selectivity of OHED hydratase

Substrate specificity of OHED was investigated using various compounds containing of carbon double bond adjacent to carboxyl group (Table 1). The results showed that all of the substrates containing aromatic ring (cinamic acid, caffeic acid, p-coumaric acid, THCA, crotonic acid, cis–maleic acid, trans-fumarate and L-malate) were not catalyzed by OHED hydratase. These results can be speculated that the aromatic ring moiety of substrate may not be able to bind enzyme active site. In case of aliphatic substrate, only trans-fumarate could be catalyzed by OHED hydratase to produce malate. When the cis isomer of fumarate, cis-maleic acid, was used as substrate, the enzyme could not convert to form new product. This indicates that OHED hydratase has a very high stereo-selectivity. The enzyme was unable to use trans-crotonic acid as substrate, although the overall molecular structure of trans-crotonic acid composed of four-carbon atom and one double bond adjacent to carboxyl group similarly to the trans-fumarate. One difference in having only one carboxylic group of trans-crotonic acid compared to the trans-fumarate resulted in noncatalyzed reaction. The results may indicate that the enzyme prefers substrate containing of two carboxyl groups at both

end of molecular structure resembling to native substrate 2-oxo-hepta-3-ene-1,7-dioic acid (OHED).

In case of HpcG, a homologue of OHED hydratase, the reaction mechanism has been proposed based on the investigation using native substrate and intermediate in Z-isomer (Izumi Rea et al. 2007). This z-isomer intermediate was also proposed in MhpD reaction of cis-2-ketopent-3-enoic acid (Pollard Bugg 1998). In Figure 5A The native substrate of HpcG (1) was tautomerized to enol form (2) which can spontaneously decay to 3E-isomer (3). This compound cannot be proceeded to product (5) by HpcG reaction. These might be the steric effect of carboxylate group that come close together with trans-formation (3). The alcohol product (5) was generated by HpcG and proposed that 3Z-isomer intermediate (4) was occurred during the reaction process. So the actual substrate of HpcG might be stable with enol form and oxyanion can coordinate to metal ion cofactor.

So, it can indicate that the geometric isomer of intermediate of reaction catalyzed by OHED hydratase may be different from HpcG and MhpD. The reverse reaction of OHED was carried out using 50% racemic compound of D,L-malate and L-malate as substrates. The production of fumarate using L-malate as substrate was higher than D,L-malate about 50% conversion (Figure 3.12). So the reverse reaction of OHED hydratase prefer L-configuration rather than D-configuration. It also may indicate that the product of forward reaction is L-malate. In GlaB, only the (-)-enantiomer of product (4-carboxy-4-hydroxy-2-oxoleatedipate, CHA) was produced for hydration reaction. Similarly, in reverse reaction, the enzyme could dehydrate only the (-)-enantiomers (Mazurkewich Brott et al. 2016).

The kinetic studied and catalytic efficiency of OHED hydratase

Normally, most of hydratases in aromatic degradation pathway have a very high substrate specificity and can catalyze reaction using compounds that structure is closely related to their native substrate. Most of them catalyze reaction using native substrate with catalytic efficiency (k_{cat}/K_m) of 11.4 x 10^{-6}, 1.23 x 10^{6}, 2.6 x 10^{6} and 1.1 x 10^{7} $M^{-1}s^{-1}$ reported in BphH, GalB, LigJ and MhpD, respectively (Wang and Seah 2005, Mazurkewich Brott et al. 2016, Hogancamp Mabanglo et al. 2018, Adachi Izumi et al. 2006). In GalB, steady state kinetics of hydration reaction were studied using different substrates with relate structure as 4-carboxy-2-hydroxy-muconate (CHM), (4- carboxy-2-hydroxypenta-2,4-dienoleatete (CHPD), 4-carboxy-4-hydroxy-2-oxoleatedipate (CHA) and 4-hydroxy-4-methyl-2-oxoglutarate (HMG) and the catalytic efficiency (k_{cat}/K_m) were

determined as 8.12 x 10^5, 3.97 x 10^3, 7.91 x 10^4 and 3.61 x 10^2 $M^{-1}s^{-1}$, respectively. Although chemical structure of CHPD and CHM were similar to the chemical structure to native substrate, but the catalytic and binding ability were decreasing around 200-fold (Mazurkewich Brott et al. 2016). This is consistent to data reported in nitrile hydratase and BphH hydratase, the catalytic efficiency of substrate analogue was lower than native substrate (Seiffert Ullmann et al. 2007, Wang and Seah 2005).

In our system, the steady state kinetic parameters of hydration and dehydration reaction using trans-fumarate and L-malate were determined. The catalytic efficiency (k_{cat}/K_m) of hydration reaction (forward reaction) was determined as 41.5 ± 0.95 s^{-1} (K_m = 1.22 ± 0.07 x 10^{-5} M, V_{max} = 1.27 ± 0.02 x 10^{-8} M s^{-1} and kcat = 5.07 ± 0.07 x $10^{-4}s^{-1}$). The catalytic efficiency of OHED hydratase is very low compared to other hydratases and were about 1.90 x 10^4 and 6.08 x 10^4 folds lower than the MhpD and GalB respectively. It might be due to the trans-fumarate is not native substrate of OHED hydratase and this reaction is not dependent on metal cofactor, without participating of metal activation can lead to a low efficiency. The catalytic efficiency of reverse reaction (k_{cat}/K_m) was determined as 1.26 ± 0.38 s^{-1} (K_m = 1.29 ± 0.04 x 10^{-4} M, V_{max} = 4.07 ± 0.03 x 10^{-9} M s^{-1} and k_{cat} = 1.63 ± 0.02 x 10^{-4} s^{-1}). The results indicate that the forward reaction is faster than the reverse reaction about 30 folds and forward reaction has lower K_m than the reverse reaction about 10 folds. This result is consistent to the previous report of GalB reaction, in which the catalytic efficiency of forward reaction was 3 folds higher than the reverse reaction (Mazurkewich Brott et al. 2016).

Conclusion

OHED hydratase from *A. baumannii* was successfully overexpressed as a soluble recombinant enzyme in *E. coli* overexpression system using auto-induction media (ZYM) with yielding of 40 g cell/4 L. The OHED hydratase could be purified through 3 steps of purification including 0.2% PEI precipitation, 10-30% ammonium sulfate precipitation and DEAE column chromatography and yielded 1 g/ 4 L of purified enzyme with more than 90% purity. The oligomeric state of purified OHED hydratase showed the native conformation of decameric enzyme with subunit molecular mass around 29.7 kDa. Metal analysis of OHED hydratase using MP-AES and ICP-OES techniques indicated that various divalent metals were found in purified enzyme, including Mn^{2+} Zn^{2+} Ca^{2+} and Mg^{2+}. Thermostability determined in purified enzyme, apo-enzyme and metal substituted apo-enzyme showed similar melting temperature (Tm) at around 57˚C, except for Zn^{2+} ion which decreased Tm to 42˚C. Optimal temperature of

purified OHED hydratase activity was observed at around 40˚C and the pH rate profile showed optimal pH at 7.0. The information from enzyme activity assay using trans-fumarate as substrate and thermal shift assay can indicate native cofactor of OHED hydratase as Mn^{2+}, since it can occupy the apo enzyme better than other metal ions without decreasing thermal stability of enzyme. The OHED hydratase did not require metal cofactor to catalyze reaction when using trans-fumarate as substrate. The water activation required in metal independent activity of OHED hydratase with trans-fumarate substrate was proposed to be enabled by active site amino acid residue.

Substrate specificity of OHED was investigated using various compounds containing of carbon double bond adjacent to carboxyl group. The results showed that all substrates containing aromatic ring were not catalyzed by OHED hydratase. The enzyme preferred substrate containing of two carboxyl groups at both end of structure. The enzyme had high stereo-selectivity as selectively catalyzed only trans-fumarate to from L-malate. The steady-state kinetic parameters of the hydration and dehydration reaction catalyzed by OHED hydratase using trans-fumarate and L-malate were determined. The OHED hydratase can faster catalyze forward reaction than the reverse reaction about 30-fold. The kinetic parameters of hydration reaction (forward reaction) were catalytic efficiency (k_{cat}/K_m) of 41.5 ± 0.95 M^{-1} s^{-1}, K_m of 1.22 ± 0.07 x 10^{-5} M, and k_{cat} of 5.07 ± 0.07 x 10^{-4} s^{-1}. While, the kinetic parameters of reverse reaction were catalytic efficiency (k_{cat}/K_m) of 1.26 ± 0.38 M^{-1} s^{-1}, K_m of 1.29 ± 0.04 x 10^{-4} M, and k_{cat} of 1.63 ± 0.02 x 10^{-4} s^{-1}.

References:

1. Adachi, T., Izumi, A., Rea, D., Park, S.Y., Tame, J.R. and Roper, D.I., 2006. Expression, purification and crystallization of 2-oxo-hept-4-ene-1, 7-dioate hydratase (HpcG) from Escherichia coli C. Acta Crystallographica Section F: Structural Biology and Crystallization Communications, 62(10), pp.1010-1012.
2. Beinert, H., Kennedy, M. C., Stout, C. D.(1996) A conitase as iron–sulfur protein, enzyme, and ironregulatory protein. *Chem. Rev*. 96, 2335–2373.
3. Bevers, L.E., Pinkse, M. W. H, Verhaert, P. D. E. M., Hagen, W. R.(2009). Oleate hydratase catalyzes the hydration of a nonactivated carbon–carbon bond. *J. Bacteriol.* 191, 5010–5012.
4. Bicas, J. L., Fontanille, P., Pastore, G. M., Larroche, C.(2010). A bioprocess for the production of high concentrations of R-(+)-α-terpineol from R-(+)-limonene. *Process Biochem*. 45, 481–486.
5. Bradford, M. M. (1976) A rapid and sensitive method for the quantitative of microgram quantities of protein using the principle of protein-dye binding. *Anal. Biochem.*72, 248-254.
6. Brodkorb, D., Gottschall, M., Marmulla, R., Lüddeke, F., Harder, J.(2010) Linalool dehydrataseisomerase, a bifunctional enzyme in the anaerobic degradation of monoterpenes. *J. Biol. Chem*. 285, 30436–30442.
7. Bujacz, G., Alexandratos, J., Wlodawer, A., Merkel, G., Andrake, M., Katz, R.A. and Skalka, A.M., 1997. Binding of different divalent cations to the active site of avian sarcoma virus integrase and their effects on enzymatic activity. *Journal of Biological Chemistry*, 272(29), pp.18161-18168.
8. Burks, E. A., Johnson, Jr. W. H., Whitman, C. P. (1998). Stereochemical and Isotopic Labeling Studies of 2-Oxo-hept-4-ene-1,7-dioate Hydratase: Evidence for an Enzyme-Catalyzed Ketonization Step in the Hydration Reaction. *Journal of the American Chemical Society*. 120, 7665-7675.
9. Chiba, M. and Kikuchi, M., 1984. The in vitro effects of zinc and manganese on δ-aminolevulinic acid dehydratase activity inhibited by lead or tin. *Toxicology and applied pharmacology*, 73(3), pp.388-394.
10. Cramp, R.A. and Cowan, D.A., 1999. Molecular characterisation of a novel thermophilic nitrile hydratase. *Biochimica et Biophysica Acta (BBA)-Protein Structure and Molecular Enzymology*, 1431(1), pp.249-260.
11. Fukasawa, K.M., Hata, T., Ono, Y. and Hirose, J., 2011. Metal preferences of zinc-binding motif on metalloproteases. *Journal of amino acids*, 2011.

12. Hanson, K. R., Rose, I. A.(1963). The absolute stereochemical course of citric acid biosynthesis. *Proc. Natl. Acad. Sci. U. S. A*. 50, 981–988.
13. Hara, H., Masai, E., Katayama, Y., Fukuda, M. (2000). The 4-Oxalomesaconate Hydratase Gene, Involved in the Protocatechuate 4,5-Cleavage Pathway, Is Essential to Vanillate and Syringate Degradation in *Sphingomonas paucimobilis* SYK-6. *Journal Of Bacteriology*, 182, 6950–6957.
14. Harayama, S., Rekik, M., Ngai, K-L., Ornston, L. N.(1989). Physically Associated Enzymes Produce and Metabolize 2-Hydroxy-2,4-Dienoate, a Chemically Unstable Intermediate Formed in Catechol Metabolism via meta Cleavage in Pseudomonas putida. J. Bacteriol, 171, p. 6251-6258.
15. Hiltunen , J.K., Qin, Y-M.(2000) β-Oxidation-strategies for themetabolism of a wide variety of acyl-CoA esters. *BBA - Molecular and Cell Biology of Lipids.*1484, 117–128.
16. Hogancamp, T.N., Mabanglo, M.F. and Raushel, F.M., 2018. Structure and Reaction Mechanism of the LigJ Hydratase: An Enzyme Critical for the Bacterial Degradation of Lignin in the Protocatechuate 4, 5-Cleavage Pathway. Biochemistry, 57(40), pp.5841-5850.
17. Holland, H.L., Gu, J-X.(1998). Preparation of (R)-3-hydroxy-3-alkylbutanolides by biocatalytic hydration of 3-alkyl-2-butenolides using Rhodococcus rhodochrous. *Biotech Lett*. 20,1125–1126.
18. Izumi, A., Rea, D., Adchi, T., Unzai, S., Park, S-Y., Roper, D. I., Tame, J. R. H.(2007) Structure and mechanism of HpcD, ahydratase in the Homoptotocatechuate Degradation pathway of Escherichia coli. *J. Mol. Biol*. 370, 899-911.
19. Jin, J., Hanefeld, U. (2011). The selective addition of water to C=C bonds; enzymes are the best chemists. *Chem. Commun*. 47, 2502-2510.
20. Johnson, Jr. W. H., Stack, T. M. M. Taylor, S. M., Burks, E. A. Whitman, C. P. (2016). Stereochemical Consequences of Vinylpyruvate Hydratase-Catalyzed Reactions. *Biochemistry*. 55, 4055-4064.
21. Laitaoja, M., Valjakka, J. and Janis, J., 2013. Zinc coordination spheres in protein structures. *Inorganic chemistry*, 52(19), pp.10983-10991.
22. Lamartiniere, C. A., Braymer, H. D., Larson, A. D.(1970). Purification and characterization of fumarase from Pseudomonas putida. *Arch Biochem Biophys*. 141, 293–302.

23. Liao, R-Z., Himo, F.(2011). Theoretical study of the chemoselectivity of tungsten-dependent acetylene hydratase. *ACS Catal.*1, 937–944.
24. Lloyd, S. J., Lauble, H., Prasad, G.S., Stout, C.D.(1999). The mechanism of aconitase: 1.8 Å resolution crystal structure of the S642A:citrate complex. *Protein Sci* . 8, 2655–2662.
25. Maneiro, M., Peon, A., Lence, E., Lence, E., Otero, J.M., Raaij van, M. J., et al.(2014). Insights into substrate binding and catalysis in bacterial type I dehydroquinase. *Biochem. J.* 462, 415–424.
26. Maresca, J.A., Graham, J. E., Bryant, D. A. (2008). The biochemical basis for structural diversity in the carotenoids of chlorophototrophic bacteria. *Photosynth Res*. 97, 121–140.
27. Mazurkewich, S., Brott, A. S., Kimber, M. S., Seah, S. Y. K. (2016) Structural and kinetic characterization of the 4-carboxy-2-hydroxymuconate hydratase from the gallate and protocatechuate 4,5-cleavage pathways of Pseudomonas putida KT2440. *The Journal of Biological Chemistry*. 291, 7669-7686.
28. Michielsen, M.J.F., Frielink, C., Wijffels, R.H., Tramper, J., Beeftink, H.H.(2000). D-malate production by permeabilized *Pseudomonas pseudoalcaligenes*; optimization of conversion and biocatalyst productivity. *Journal of Biotechnology.* 79, 13-26.
29. Montgomery, M.G., Coker, A.R., Taylor, I.A. and Wood, S.P., 2010. Assembly of a 20-nm protein cage by Escherichia coli 2-hydroxypentadienoic acid hydratase. *Journal of molecular biology*, 396(5), pp.1379-1391.
30. Peieto, M. A., Diaz, E., Garcia, J. L.(1996). Molecular Characterization of the 4-Hydroxyphenylacetate Catabolic Pathway of Escherichia coli W: Engineering a Mobile Aromatic Degradative Cluster. *J. Bacteriol*,. 178. p111–120.
31. Piersma, S.R., Nojiri , M., Tsujimura , M., Noguchi , T., Odaka , M., Yohda , M., Inoue , Y., Endo . I.(2000). Arginine 56 mutation in the b subunit of nitrile hydratase: importance of hydrogen bonding to the non-heme iron center. *Journal of Inorganic Biochemistry.* 80, 283–288.
32. Pfleger, B. F., Kim, Y., Nusca, T.D., Maltseva, N., Lee, J.Y., Rath, C.M., et al.(2008). Structural and functional analysis of AsbF: origin of the stealth 3,4-dihydroxybenzoic acid subunit for petrobactin biosynthesis. *Proc. Natl. Acad. Sci. U.S.A.* 105,17133–17138.
33. Pollard, J. R., Bugg, T. D. H. (1998). Purification, characterisation and reaction mechanism of monofunctional 2-hydroxypentadienoic acid hydratase from *Escherichia coli*. *Eur. J. Biochem*. 251, 98-106.

34. Roszak, A. W., Robinson, D. A., Krell, T., Hunter, I. S., Fredrickson, M., Abell, C., et al. (2002). The structure and mechanism of the type II dehydroquinase from Streptomyces coelicolor. *Structure*. 10, 493-503.
35. Saito, N., 1967. Purification and properties of bacterial phosphopyruvate hydratase. *The Journal of Biochemistry*, 61(1), pp.59-69.
36. Sacks, W., Jensen, C. O.(1951).Malease, a hydratase from corn kernels. *J. Biol. Chem*. 192, 231–236.
37. Seiffert, G.B., Ullmann, G.M., Messerschmidt, A., Schink, B., Kroneck, P.M. and Einsle, O., 2007. Structure of the non-redox-active tungsten/[4Fe: 4S] enzyme acetylene hydratase. Proceedings of the National Academy of Sciences, 104(9), pp.3073-3077.
38. Thotsaporn, K., Tinikul, R., Maenpuen, S., Phonbuppha, J., Watthaisong, P., Chenprakhon, P., Chaiyen, P. (2016) Enzymes in the p-hydroxyphenylacetate degradation pathway of Acinetobacter baumannii. *Journal of Molecular Catalysis B: Enzymatic*. 134(B), 353–366.
39. Turbek, C.S., Smith, D. A., Schardl, C.L.(1992). An extracellular enzyme from Fusarium solani f. sp. phaseoli which catalyses hydration of the isoflavonoid phytoalexin, phaseollidin. *FEMS Microbiol Lett*. 94,187–190.
40. Tyagi, R., Eswaramoorthy, S., Burley, S.K., Raushel, F. M., Swaminathan, S.(2008). A common catalytic mechanism for proteins of the hutI family. *Biochemistry*. 47, 5608–5615.
41. Wang, P., Seah, S. Y. K. (2005). Determination of the metal ion dependence and substrate specificity of a hydratase involved in the degradation pathway of biphenyl/chlorobiphenyl. *FEBS Journal*. 272, 966–974.
42. Weaver, T., Banaszak, L.(1996). Crystallographic studies of the catalytic and a second site in fumarase C from Escherichia coli. *Biochemistry*. 35, 13955–13965.
43. Wuensch, C., Gross, J., Steinkellner, G., Gruber, K., Glueck, S.M., Faber, K.(2013) Asymmetric enzymatic hydration of hydroxystyrene derivatives. *Angew. Chem. Int. Ed. Engl*. 52, 2293–2297.

5. Output (Acknowledge the Thailand Research Fund)

5.1International Journal Publication

a) Chenprakhon, P*., Wongnate, T., Chaiyen, P. (2019) Monooxygenation of Aromatic Compounds by Flavin-Dependent Monooxygenases. *Protein Science*. 28: 8–29. (IF= 2.41)

b) Duangpummet, P., Chaiyen, P., Chenprakhon P*. (2019) Lipase-Catalyzed Esterification: An Inquiry-Based Laboratory Activity To Promote High School Students' Understanding and Positive Perceptions of Green Chemistry. *Journal of Chemical Education*. 96 (6), 1205-1211 (IF= 1.758)

C) Pitsawong, W., Chenprakhon, P., Dhammaraj, T., Medhanavyn, D., Sucharitakul, J., Tongsook, C., van Berkel, W.J., Chaiyen, P. and Miller, A.F., 2020. Tuning of pKa values activates substrates in flavin-dependent aromatic hydroxylases. *Journal of Biological Chemistry*, 295(12), 3965-3981.

d) Recombinant expression, purification, biochemical characterization, and mechanistic investigation Of 2-oxo-hept-3-ene-1,7-dioic acid hydratase from p-hydroxyphenylacetate degradation pathway of *Acinetobacter baumannii* **(In preparation)**

5.2 Others e.g. national journal publication, proceeding, international conference, book chapter, patent

a) Chenprakhon, P*, Pimviriyakul, P., Tongsook, C. and Chaiyen, P., 2020. Phenolic hydroxylases. The Enzymes, 47, pp.283-326.

6. Appendix

Reprint of International Journal Publications

6.1) Chenprakhon, P*., Wongnate, T., Chaiyen, P. (2019) Monooxygenation of Aromatic Compounds by Flavin-Dependent Monooxygenases. Protein Science. 28: 8–29.

6.2) Duangpummet, P., Chaiyen, P., Chenprakhon P*. (2019) Lipase-Catalyzed Esterification: An Inquiry-Based Laboratory Activity To Promote High School Students' Understanding and Positive Perceptions of Green Chemistry. Journal of Chemical Education. 96(6), 1205-1211.

6.3 Pitsawong, W., Chenprakhon, P., Dhammaraj, T., Medhanavyn, D., Sucharitakul, J., Tongsook, C., van Berkel, W.J., Chaiyen, P. and Miller, A.F., 2020. Tuning of pKa values activates substrates in flavin-dependent aromatic hydroxylases. *Journal of Biological Chemistry*, 295(12), 3965-3981.